

Testing the Concept of Quark-Hadron Duality with the ALEPH τ Decay Data

B.A. Magradze

Received: date / Accepted: date

Abstract We propose a modified procedure for extracting the numerical value for the strong coupling constant α_s from the τ lepton hadronic decay rate into non-strange particles in the vector channel. We employ the concept of the quark-hadron duality specifically, introducing a boundary energy squared $s_p > 0$, the onset of the perturbative QCD continuum in Minkowski space [1, 2, 3]. To approximate the hadronic spectral function in the region $s > s_p$, we use Analytic Perturbation Theory (APT) up to the fifth order. A new feature of our procedure is that it enables us to extract from the data simultaneously the QCD scale parameter $\Lambda_{\overline{\text{MS}}}$ and the boundary energy squared s_p . We carefully determine the experimental errors on these parameters which come from the errors on the invariant mass squared distribution. For the $\overline{\text{MS}}$ scheme coupling constant, we obtain $\alpha_s(m_\tau^2) = 0.308 \pm 0.014_{\text{exp.}}$. We show that our numerical analysis is more stable against higher-order corrections than the standard one. The extracted value for the duality point s_p is found surprisingly stable against perturbation theory corrections $s_d = 1.71 \pm 0.05_{\text{exp}} \pm 0.00_{\text{th}}$ GeV². Additionally, we recalculate the “experimental” Adler function in the infrared region using final ALEPH results. The uncertainty on this function is also determined.

Keywords tau lepton decay · renormalization group equation · perturbation theory data analysis

1 Introduction

The hadronic τ decays serves as an ideal laboratory for testing quantum chromodynamics (QCD) in a relatively low energy regime. In the past, various techniques (fixed order perturbation theory, contour improved perturbation theory, effective charge approach, renormalons, dispersive approach) have been devised to improve the reliability of the predictions of the theory for the τ system. In this boundary area of the energy, perturbative ideas are still applicable due to relatively large mass of the τ lepton,

B.A. Magradze

Andrea Razmadze Mathematical Institute of I. Javakhishvili Tbilisi State University, 2, University st., 0186 Tbilisi, Georgia
E-mail: magr@rmi.acnet.ge

while non-perturbative effects are expected to be small. Usually, they are under control within Wilson Operator Product Expansion (OPE) [4]. It is known that the main calculational tool in perturbative QCD (pQCD) the renormalization group improved perturbation theory augmented with the OPE can not be used locally in the time-like region even at high energy. Fortunately, this problem has been resolved in earlier work [5] by means of the idea of the quark-hadron duality. This enabled one to employ the QCD perturbation theory in Minkowski region to calculate some global (inclusive) quantities like τ lepton decay rate. Although the quark-hadron duality cannot be justified rigorously from the first principles, in practice this idea works good enough. Using the duality, an accurate description of the τ lepton decay data was achieved (see the seminal work [6] and the literature therein). However, one should always keep in mind that the duality between a physical quantity and its quark-gluon perturbation theory representation is only approximative and thus it must inevitable be violated (see the review [7] and the literature therein). To identify general mechanism of possible Duality Violations (DVs), special QCD inspired models for the hadronic spectral functions (e.g. the instanton-based and resonance-based models [7] as well as the models motivated by the large N_c limit of the theory [8]) have been studied. In these models DVs in fact occur. Presumably, DVs arise due to the lack of the convergence of the OPE on the Minkowski axis. If this is the case, then the analytical continuation of the truncated OPE series from the Euclidean region to the physical axis is questionable [7].

In recent years, the accuracy of the measurements of the observables of the τ lepton system has been essentially improved (for the recent results of the ALEPH collaboration see [9,10,11,12]). This enables one to extract the parameters of the standard model from τ data with very high precision. Of particular interest is the numerical value of the strong coupling constant α_s . Admittedly, one of the most precise determinations of the strong coupling constant comes from the analysis of the τ data (for most recent results see [12]). An independent low-energy highest-precision determination of α_s comes from lattice QCD simulations combined with experimental data for hadron masses [13]. These two highest-precision determinations extrapolated to the Z mass yield

$$\alpha_s(M_z^2) = 0.1212 \pm 0.0011 \quad (\tau \text{ decay}) \quad (1)$$

$$\alpha_s(M_z^2) = 0.1170 \pm 0.0012 \quad (\text{lattice}). \quad (2)$$

Note that the agreement between these two results, with the errors quoted, is not good. They differ from each other by about 2.6 standard deviations. Furthermore, the lattice determination is closer to $\alpha_s(M_z^2)$ values obtained from high energy experiments. Thus, the reliability of the estimates from the τ -lepton data has been called in question [12, 14,15,16,17,18,19,20,21]. The small but still significant non-perturbative effects have been included into analysis [18,21]. On the one hand, the impact of the higher order terms of the OPE (neglected in the standard analyzes) has been estimated [14,15,16,17]. It was confirmed that their influence on the extracted value of α_s is not small in the separate vector and axial vector channels. To suppress these contributions in the finite energy sum rule the so-called pinched weights introduced [14,15,16,17]. An independent estimation of possible non-perturbative corrections to the finite energy sum rule (direct instantons, duality violation and tachyonic gluon mass) which cannot be described within OPE can be found in [18]. To estimate systematic effects from DVs, recently the authors of [12] have analyzed the ALEPH τ data for the V+A spectral function using two different models of DVs. These models were previously considered in [7]. It was confirmed (within this models) that DVs effects in this channel

are completely negligible. However, this problem has been reconsidered in [20]. There the separate vector (V) and axial-vector (A) spectral data have been analyzed. To describe DVs coming from the region $s \geq 1.1 \text{ GeV}^2$ physically motivated models for these spectral functions have been suggested. Analyzing the τ data provided by the ALEPH collaboration, the authors of [20] have concluded that DVs are not small. An additional systematic error in the value of the coupling constant coming from DVs has been estimated on the level $\delta\alpha_s(m_\tau^2) \approx 0.003 - 0.010$.

As is well known, in the time-like region the renormalization group (RG) invariance cannot be used unambiguously. Usually, the QCD corrections to the τ lepton decay rate R_τ is expressed via the contour integral of the associated Adler function multiplied by the known weight function. This representation is valid owing to special analyticity structure of the corresponding exact current-current correlation function. The Adler function is represented via the truncated perturbation theory series and the integral is taken over the circle of radius m_τ^2 (m_τ stands for the τ -lepton mass) in the complex energy squared plane [6]. One possibility is to integrate term-by-term the truncated perturbation theory series over the contour and then perform the RG improvement. This approach is referred to as fixed order perturbation theory (FOPT). Alternatively, one can insert the RG improved truncated series for the Adler function inside the contour integral and then perform the integral. This approach suggested in [22,23,24] was termed contour improved perturbation theory (CIPT). The advantage of CIPT is that it enables to resume some higher-order contributions to the rate. These two approaches lead to differing results. The values of α_s extracted from τ decays employing CIPT have always been higher. A detailed comparison of these two approaches may be found in recent works [25,26]. A practical review of various approaches to the τ decay rate may be found in [11].

The inclusive quantity like hadronic τ decay rate may be accurately described within pure perturbative approach, provided the DVs are small. Indeed, in the V+A channel, the nonperturbative power suppressed contributions described by the OPE (continued analytically to the time-like region) have been estimated to be small [6,12,18]. However, the large value of the running coupling parameter at the τ lepton mass scale leads to the large renormalization scheme dependence of perturbative predictions. To reduce this dependence various resummation techniques have been developed (see, for example, [27,28,29]). In [27], the V+A τ -lepton decay data was analyzed within a modified extraction procedure based on the effective charge approach. The numerical analysis has been performed in the internal renormalization scheme of the τ system and then the result was translated into the $\overline{\text{MS}}$ scheme using renormalization scheme transformation. This procedure yields smaller value for the coupling constant. Similarly, in [28] and [29] in calculations of the τ decay rate the minimal sensitivity and effective charge schemes were used. In this way the reliability of the estimates for the coupling constant has been improved.

A serious shortcoming of the conventional perturbation theory approximations to the current-current correlation functions parameterized in terms of the running coupling is that they do not obey correct analytical properties of the corresponding exact quantities. The analytical properties are violated due to the non-physical Landau singularities of the perturbative running coupling which appear at small space-like momenta (for the analytical structure of the perturbative coupling beyond the one-loop order see [30,31,32,33]). Supposedly, these singularities may deteriorate the extracted values of the parameters [34]. This problem does not arise within dispersive or analytic approaches to pQCD. At present, several such approaches are being intensively

developed [35, 36, 37, 38, 39, 40, 41, 42, 43, 44, 45, 46, 47, 48, 49, 50, 51, 52]. In works [38] and [39], the τ lepton decay rate has been analyzed within a simple and effective dispersive technique, the Analytic Perturbation Theory (APT) (for reviews see [40, 41, 43, 46, 52]). However, the minimal analytic QCD model (the same APT) predicts, from the non-strange τ lepton decay data, too large value for the strong coupling constant, $\alpha_s(m_\tau^2) = 0.403 \pm 0.015$ [39]. The advantages and shortcomings of the three approaches to the τ decays (FOPT, CIPT and APT) were thoroughly analyzed in [44]. It should be noted that the APT as well as its generalized versions suggested more later [47, 48, 49, 50] proved to be very useful from the phenomenological point of view. A remarkable feature of these modified expansions is the better convergence and improved stability property with respect to change of the renormalization scheme. Nevertheless, one should keep in mind that an analytic approach based only on perturbation theory can not be defined unambiguously, since there is not a unique recipe for removing the Landau singularities from the running coupling.

A particular problem emerges from the observation that the QCD perturbation theory augmented with the OPE fail to describe the detailed infrared behavior of the Adler function associated with the τ decay rate [3]. To treat this problem a more general framework is required. A suitable theoretical framework was suggested in [3]. There the hadronic non-strange vector spectral function $v_1(s)$ ¹ was represented by a simple *ansatz*

$$v_1(s) \approx \theta(s_p - s)v_1^{\text{np}}(s) + \theta(s - s_p)v_1^{\text{pQCD}}(s), \quad (3)$$

where $v_1^{\text{pQCD}}(s)$ is the perturbation theory approximation to the spectral function and s_p is the onset of perturbative continuum², an infrared boundary in Minkowski region above which we trust pQCD. The non-perturbative component of the spectral function $v_1^{\text{np}}(s)$ was described by a resonance based model (“the lowest meson dominance approximation to large- N_c QCD”). Using this model the authors of [3] have achieved correct matching in the intermediate region between the pQCD and Chiral Perturbation Theory predictions for the Adler function³. To compare the Adler function evaluated from (3) to the experiment the authors of [3] have also constructed the “experimental” spectral function

$$v_1^{\text{“exp”}}(s) = \theta(s_p - s)v_1^{\text{exp}}(s) + \theta(s - s_p)v_1^{\text{pQCD}}(s), \quad (4)$$

where $v_1^{\text{exp}}(s)$ is the genuine experimental part of the total “experimental” spectral function which is measured with high precision by ALEPH [9, 53] and OPAL [54] collaborations in the range $0 < \sqrt{s} < m_\tau = 1.777 \text{ GeV}$. Formula (4) extends the spectral function beyond the range accessible in the experiment. Formulas (3) and (4) provide practical realizations of the concept of the quark-hadron duality (see the original works [1, 2]). The *ansatz* (3) may be considered as an alternative for the truncated OPE in Minkowski region. The conventional formulation of the duality may be recovered from formulas (3) or (4) by taking the limit $s_p \rightarrow 0$ and introducing the OPE contributions⁴. Note that, the non-perturbative corrections to the spectral function described by model (3) are essentially confined in the low energy region $0 < s < s_p$.

¹ We use the normalization of the spectral function with the naive parton prediction $v_{1,\text{naive}} = 1/2$.

² The inequality $0 < s_p < m_\tau^2$ is assumed.

³ The infrared behaviour of the Adler function was also correctly described within APT [45]. However, to reproduce the τ data, APT requires large effective quark masses.

⁴ Strictly speaking this is true if the perturbation theory component of the spectral function $v_1^{\text{pQCD}}(s)$ is evaluated within FOPT or APT.

In this paper we concentrate on formula (4). Our aim is to utilize the total information encoded in this representation. We recall that the authors of [3] have used *ansatz* (4) to extract the numerical value for the parameter s_p from the experimental data. For the $\overline{\text{MS}}$ scheme scale parameter (for the three active flavours) they used the estimate

$$\Lambda_{\overline{\text{MS}}} = (372 \pm 72) \text{ MeV}. \quad (5)$$

The QCD component of the spectral function, $v_1^{\text{pQCD}}(s)$, was determined from the order $\mathcal{O}(\alpha_s^3)$ approximation to the Adler function. The approximation was constructed in terms of the exact numeric two-loop running coupling constant, normalized at the scale s_p . The experimental component $v_1^{\text{exp}}(s)$ was reconstructed from the ALEPH collaboration data obtained in 1999 [53]. Note that the estimate (5) is close to the ALEPH result for the scale parameter obtained for that time

$$\Lambda_{\overline{\text{MS}}} = (370 \pm 51) \text{ MeV}.$$

However, these two results for $\Lambda_{\overline{\text{MS}}}$ should not be compared. The final result of the collaboration for the coupling constant corresponds to the average of the two values obtained within the FOPT and CIPT approaches, while authors of [3] used only FOPT. Furthermore, in the ALEPH analysis the estimate for $\mathcal{O}(\alpha_s^4)$ term was also included, while the QCD scale parameter was extracted using the exact (numeric) four-loop running coupling. Using the *ansatz* (4) the authors of [3] have derived consistency condition from the OPE, an equation relating the parameters s_p and $\Lambda_{\overline{\text{MS}}}$. From this equation, with the estimate (5), they have found that

$$s_p = (1.60 \pm 0.17) \text{ GeV}^2. \quad (6)$$

Usually, it is more convenient to compare the time-like experimental data with theory via the Adler function, the object determined in the space-like region [55]⁵

$$D(Q^2) = Q^2 \int_0^\infty \frac{2v_1(s)ds}{(s+Q^2)^2}, \quad (7)$$

for this quantity reliable approximations are constructed in pQCD, in massless [56, 57, 58, 59, 60] as well as in massive cases [60, 55]. The “experimental” Adler function is obtained by inserting *ansatz* (4) into integral (7)

$$D_{\text{“exp”}}(Q^2) = D_{\text{exp}}(Q^2, s_p) + D_{\text{pQCD}}(Q^2, s_p), \quad (8)$$

where the experimental and perturbation theory components of the total “experimental” Adler function are defined as

$$D_{\text{exp}}(Q^2, s_p) = Q^2 \int_0^{s_p} \frac{2v_1^{\text{exp}}(s)ds}{(s+Q^2)^2}, \quad D_{\text{pQCD}}(Q^2, s_p) = Q^2 \int_{s_p}^\infty \frac{2v_1^{\text{pQCD}}(s)ds}{(s+Q^2)^2}. \quad (9)$$

Note that the “experimental” Adler function is not wholly experimental quantity, since it depends also on the theoretical component $D_{\text{pQCD}}(Q^2, s_p)$. The latter may be calculated using different theoretical approaches. For example, one may apply FOPT or APT. Furthermore, the result will depend on the higher order corrections to the β -function and to the Adler function. In the past years, the “experimental” Adler function

⁵ we use notation $q^2 = -Q^2$ and $Q^2 > 0$ for space-like momenta

was employed for testing various theoretical approximations to the Adler function [3, 45, 47].

In view of appearance of final ALEPH data in 2005 [9, 10] it is worthwhile to recalculate the “experimental” Adler function. In this paper, we will use different strategy for extracting numerical values of the parameters from the data. The distinguishing feature of our analysis is that we will determine both parameters ($\Lambda_{\overline{\text{MS}}}$ and s_p) self-consistently. Secondly, we pay particular attention to the estimation of the experimental errors on the parameters and Adler function. Furthermore, we will use a dispersive approach⁶.

In Sect. 2 we evaluate the perturbative component of the hadronic spectral function up to order $\mathcal{O}(\alpha_s^5)$ within the dispersive approach. Then, we derive a transcendental system of equations for the parameters $\Lambda_{\overline{\text{MS}}}$ and s_p . The first equation of the system follows from the OPE for the current-current correlation function in the limit of massless quarks. The second equation for the parameters is a consequence of the quark-hadron duality implemented by means of the *ansatz* (4); perturbation theory is used to calculate the decay rate of the τ -lepton into hadrons of invariant mass larger than $\sqrt{s_p}$. In Sect. 3 we solve the system of equations for the parameters numerically. To determine the empirical contributions in these equations, we employ the final ALEPH data on the non-strange vector invariant mass squared distributions which are available in [10]. To test the stability of the numerical results against the QCD perturbative corrections, we use different approximations to the Adler function from order $\mathcal{O}(\alpha_s)$ to order $\mathcal{O}(\alpha_s^5)$. This enables us to determine the indicative theoretical errors [27] on the extracted numerical values of the parameters. Our approach, which we refer to as APT⁺, is compared with the standard CIPT. In the most of the calculations, we use the four-loop running coupling. In Sect. 4, we present numerical results for the “experimental” Adler function obtained from the final ALEPH data. The values and associated experimental errors of the function are tabulated in the region $Q = 0 - 1.5$ GeV. Our conclusions are given in Sect. 5. In Appendix A we give some practical formulas obtained from the explicit (series) solution to the higher order RG equation. The statistical errors on the parameters are carefully estimated in Appendix B. In Appendix C we present some required results obtained within standard CIPT.

2 Theoretical Framework

The main quantity of interest for following analysis is the Adler function associated with the vector current two-point correlator. The perturbative expansion of this function in the limit of vanishing quark masses reads [25]

$$D(Q^2) = \sum_{n=0}^{\infty} a_s^n(\mu^2) \sum_{k=1}^{n+1} k c_{n,k} L^{k-1} \quad \text{where} \quad L \equiv \ln \frac{Q^2}{\mu^2}, \quad (10)$$

$a_s(\mu^2) = \frac{\alpha_s(\mu^2)}{\pi}$ with $\alpha_s(\mu^2)$ being the strong coupling constant renormalized at the scale μ . Since the Adler function is a physical quantity, it satisfies a homogenous RG equation. This fact enables us to choose $\mu^2 = Q^2$. Then the expansion (10) may be

⁶ The difference between our framework and APT of Shirkov and Solovtsov is clarified in Sect. 2.

reexpressed as an asymptotic expansion in powers of the running coupling $\alpha_s(Q^2)$

$$D_{\text{RGI}}(Q^2) = \sum_{k=0}^{\infty} d_k \left(\frac{\alpha_s(Q^2)}{\pi} \right)^k, \quad (11)$$

where $d_n = c_{n,1}$ and the subscript “RGI” refers to the renormalization group improved perturbation theory. The first two coefficients in series (11) are universal $d_0 = d_1 = 1$. The coefficients of order α_s^2 and α_s^3 in the $\overline{\text{MS}}$ scheme have been calculated about thirty and fifteen years ago [56, 57, 58]. Recently, the authors of [59] have calculated the coefficient d_4 in the case of massless quarks by using powerful computational techniques. The known higher order coefficients in the $\overline{\text{MS}}$ scheme for $n_f = 3$ quark flavours take values $d_2 \simeq 1.6398$, $d_3 \simeq 6.3710$ and $d_4 \simeq 49.0757$.

In practice the series (11) should be truncated. The obtained approximations to the Adler function do not obey correct cut-plane analyticity properties of the exact function because of the non-physical “Landau singularities” which present in the perturbative running coupling. The exact Adler function $D(z)$ ($z = Q^2 = -q^2$) is known to be analytic except the cut running along the negative real axis. This fact enables us to calculate the hadronic non-strange vector spectral function from the Adler function via the contour integral

$$v_1(s) = \frac{1}{4\pi i} \oint_{-s-i0}^{-s+i0} \frac{D(z)}{z} dz, \quad (12)$$

where the path of integration, connecting the points $-s \mp i0$ on the complex z -plane, avoids the cut running along the real negative axis. The integral being traversed in a positive (anticlockwise) sense. In this paper we shall assume, without loss of generality, that the approximation (11) to the Adler function has only one non-physical singularity located on the positive real axis. This is the case, for the exact (explicitly solved) two-loop order running coupling in $\overline{\text{MS}}$ like renormalization schemes⁷. On the other hand, a running coupling at higher orders may be expanded in powers of the exact (explicitly solved) two-loop order coupling [61, 62]

$$\alpha_s^{(\text{k-loops})}(Q^2) = \sum_{n=1}^{\infty} \mathcal{C}_n^{(k)} \alpha_s^{(\text{two-loops})n}(Q^2)|_{\text{exact}}, \quad (13)$$

where the numerical coefficients $\mathcal{C}_n^{(k)}$ are determined in terms of the β -function coefficients (see Appendix A). It was shown in [33] that this series has a sufficiently large radius of convergence in the space of the coupling constants, and its partial sums provide very accurate approximations to the exact k -th order ($k > 2$) coupling in the complex Q^2 plane. To construct accurate approximations to the running coupling for small values of $|Q|^2$, one should keep sufficiently large number of terms in the partial sum. The Adler function evaluated with this approximation to the coupling has only one non-physical singularity located on the positive Q^2 -axis. The corresponding cut runs along the finite interval of the positive Q^2 -axis. Nevertheless, formula (12) is still valid provided that the integration contour avoids the physical as well as non-physical cut.

⁷ The analytic structure of the explicit exact solution to the RG equation at the two-loop order has been determined in [30, 31, 32].

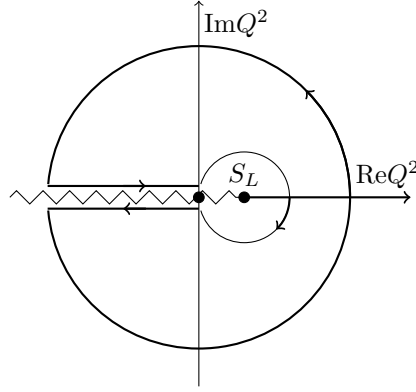


Fig. 1 Contour in the complex Q^2 plane used in the Cauchy relation (15). Branch points on the real axis are represented by the blobs and brunch cuts by the zigzagging line.

Let us separate out the parton level term from the perturbative Adler function

$$D_{\text{RGI}}(Q^2) = 1 + d_{\text{RGI}}(Q^2) : \quad d_{\text{RGI}}(Q^2) = \sum_{k=1}^{\infty} d_k a_s^k(Q^2), \quad (14)$$

where $a_s(Q^2) = \alpha_s(Q^2)/\pi$. As it was discussed above, the function $d_{\text{RGI}}(Q^2)$ is analytic except the cuts running along the real Q^2 -axis. The physical cut runs along the real negative semi-axis $-\infty < Q^2 < 0$, and the non-physical cut runs along the positive interval $0 < Q^2 < s_L$, where the point $Q^2 = Q_L^2 \equiv s_L > 0$ corresponds to the “Landau singularity”. We may then write a Cauchy relation

$$d_{\text{RGI}}(Q^2) = \frac{1}{2\pi i} \oint_{\Gamma} \frac{d_{\text{RGI}}(w)}{w - Q^2} dw \quad (15)$$

where the integral is taken round the closed contour Γ drawn in Fig.1. The contour consists of the arc of the circle $|Q^2 - s_L| = s_L$, straight lines parallel to the real negative Q^2 axis and passes round a big circle. Using formula (15) together with the asymptotic condition $d_{\text{RGI}}(z) \rightarrow 0$ as $|z| \rightarrow \infty$, we derive a violated dispersion relation (DR)

$$d_{\text{RGI}}(Q^2) = d_{\text{APT}}(Q^2) + d_L(Q^2) \quad (16)$$

here the function $d_{\text{APT}}(Q^2)$ satisfies the DR

$$d_{\text{APT}}(Q^2) = \frac{1}{\pi} \int_0^{\infty} \frac{\rho_{\text{eff}}(\sigma)}{\sigma + Q^2} d\sigma, \quad (17)$$

with the effective spectral density

$$\rho_{\text{eff}}(\sigma) = \text{Im}\{d_{\text{RGI}}(-\sigma - i0)\}. \quad (18)$$

It is to be noted here that the function

$$D_{\text{APT}}(Q^2) = 1 + d_{\text{APT}}(Q^2) \quad (19)$$

is the analytic image of the perturbative Adler function determined in the sense of the Analytic Perturbation Theory (APT) approach of Shirkov and Solovtsov [40,41]. The second term in (16), which violates the DR, corresponds to the contribution to the integral (15) coming from the “Landau branch cut”. It is represented by the contour integral

$$d_L(Q^2) = -\frac{1}{2\pi i} \oint_{C_L^+} \frac{d_{\text{RGI}}(\zeta)}{\zeta - Q^2} d\zeta, \quad (20)$$

taken round the circle $\{\zeta : \zeta = s_L + s_L \exp(i\phi), -\pi < \phi \leq \pi\}$ in the positive (anti-clockwise) direction.

The perturbation theory approximation to the hadronic spectral function is calculated by inserting the series (14) into the inversion formula (12). An important point is that the “Landau part” $d_L(Q^2)$ does not contribute into the spectral function, provided that $s > 0$. To see this, let us evaluate this contribution to the spectral function, with the aid of formula (20),

$$\begin{aligned} 2v_1(s)|_L &= \frac{1}{2\pi i} \oint_{-s-i0}^{-s+i0} \frac{d_L(z)}{z} dz = -\left(\frac{1}{2\pi i}\right)^2 \oint_{-s-i0}^{-s+i0} \frac{dz}{z} \oint_{C_L^+} \frac{d_{\text{RGI}}(\zeta)}{\zeta - z} d\zeta = \\ &= -\frac{1}{2\pi i} \oint_{C_L^+} d_{\text{RGI}}(\zeta) \left\{ \frac{1}{2\pi i} \oint_{-s-i0}^{-s+i0} \frac{1}{z(\zeta - z)} dz \right\} d\zeta, \end{aligned} \quad (21)$$

here we have interchanged the order of integration in the repeated integral. Let us consider the integral under braces. For $\zeta \neq 0$ the integrand has two simple poles inside the contour of integration. It follows from the theorem of residues that this integral vanishes, provided $s > 0$,

$$\frac{1}{2\pi i} \oint_{-s-i0}^{-s+i0} \frac{1}{z(\zeta - z)} dz \equiv 0,$$

and the same result holds for $\zeta = 0$. We have thus found that only the “analytic component” $d_{\text{APT}}(Q^2)$ gives a finite contribution into the hadronic spectral function. Using DR (17) and inversion formula (12), one finds the expression for the spectral function in terms of the effective spectral density

$$v_1^{\text{pQCD}}(s) \equiv v_1^{\text{APT}}(s) = \frac{1}{2}(1 + r(s)), \quad (22)$$

where

$$r(s) = \frac{1}{\pi} \int_s^\infty \frac{\rho_{\text{eff}}(\sigma)}{\sigma} d\sigma. \quad (23)$$

Note that formulas (22) and (23) were previously obtained in the context of APT (see [39] and [44]). With the help of formula (22), we express the “perturbative component” of the total “experimental” Adler function in terms of the effective spectral density

$$D_{\text{pQCD}}(Q^2, s_p) = \int_{s_p}^\infty \mathcal{K}(Q^2, s)(1 + r(s)) ds \quad (24)$$

where we have introduced the notation $\mathcal{K}(Q^2, s) = Q^2/(s + Q^2)^2$. Integrating (24) by parts we obtain a more convenient representation

$$D_{\text{pQCD}}(Q^2, s_p) = \frac{Q^2}{s_p + Q^2}(1 + r(s_p)) - \frac{Q^2}{\pi} \int_{s_p}^\infty \frac{\rho_{\text{eff}}(\sigma)}{\sigma(\sigma + Q^2)} d\sigma. \quad (25)$$

Let us now evaluate power suppressed corrections to the total “experimental” Adler function (8). We may rewrite the perturbative component of the Adler function identically

$$\begin{aligned} D_{\text{pQCD}}(Q^2, s_p) &= D_{\text{APT}}(Q^2) - 2 \int_0^{s_p} \mathcal{K}(Q^2, s) v_1^{\text{APT}}(s) ds \\ &= D_{\text{RGI}}(Q^2) - d_L(Q^2) - 2 \int_0^{s_p} \mathcal{K}(Q^2, s) v_1^{\text{APT}}(s) ds, \end{aligned} \quad (26)$$

in the first line of (26) we have used the definition of the analytic image of the Adler function

$$D_{\text{APT}}(Q^2) = 1 + d_{\text{APT}}(Q^2) = 2 \int_0^\infty \mathcal{K}(Q^2, s) v_1^{\text{APT}}(s) ds, \quad (27)$$

which is easily deduced from the discussion given above. The last equality on the right of (26) follows from formula (16). The power suppressed part of the total “experimental” Adler function is determined as

$$D_{\text{p.s.}}(Q^2, s_p) = D_{\text{“exp”}}(Q^2) - D_{\text{RGI}}(Q^2). \quad (28)$$

Combining formulas (8), (16) and (26), we rewrite formula (28) in the form

$$\begin{aligned} D_{\text{p.s.}}(Q^2, s_p) &= D_{\text{exp}}(Q^2, s_p) + D_{\text{pQCD}}(Q^2, s_p) - D_{\text{RGI}}(Q^2) \\ &= \int_0^{s_p} K(Q^2, s) 2v_1^{\text{exp}}(s) ds - d_L(Q^2) - \int_0^{s_p} K(Q^2, s) 2v_1^{\text{APT}}(s) ds. \end{aligned} \quad (29)$$

From definitions (20) and (24), we obtain the asymptotic formulas, for $Q^2 \rightarrow \infty$,

$$\mathcal{K}(Q^2, s) \approx Q^{-2} + \mathcal{O}(sQ^{-4}), \quad d_L(Q^2) \approx c_L \Lambda^2 Q^{-2} + \mathcal{O}(\Lambda^4 Q^{-4}), \quad (30)$$

where Λ denotes the conventional $\overline{\text{MS}}$ -scheme QCD parameter ($\Lambda \equiv \Lambda_{\overline{\text{MS}}}$). Since the parameter s_L is proportional to Λ^2 ⁸, the coefficient c_L is a positive number independent of Λ

$$c_L = \Lambda^{-2} \frac{1}{2\pi i} \oint_{C_L^+} d_{\text{RGI}}(\zeta) d\zeta = \frac{1}{2\pi} \frac{s_L}{\Lambda^2} \int_{-\pi}^{\pi} d_{\text{RGI}}(s_L + s_L e^{i\phi}) d\phi. \quad (31)$$

Using formulas (29) and (30), we write asymptotic expansion for $D_{\text{p.s.}}(Q^2, s_p)$. It follows from the OPE that the leading term in the asymptotic expansion, proportional to Q^{-2} , vanishes if the quarks are massless. This leads to the equation⁹

$$c_L \Lambda^2 + \int_0^{s_p} 2v_1^{\text{APT}}(s) ds \equiv c_L \Lambda^2 + s_p + \int_0^{s_p} r(s) ds = \int_0^{s_p} 2v_1^{\text{exp}}(s) ds, \quad (32)$$

the first equality in Eq. (32) follows from the relation (22). Using Eq. (23), by partial integration we find

$$\int_0^{s_p} r(s) ds = s_p r(s_p) + \frac{1}{\pi} \int_0^{s_p} \rho_{\text{eff}}(\sigma) d\sigma, \quad (33)$$

here we have used the relation $sr(s) \rightarrow 0$ as $s \rightarrow 0$, which holds in every order of perturbation theory. Combining Eqs. (32) and (33), we obtain

$$c_L \Lambda^2 + s_p(1 + r(s_p)) + \frac{1}{\pi} \int_0^{s_p} \rho_{\text{eff}}(\sigma) d\sigma = \int_0^{s_p} 2v_1^{\text{exp}}(s) ds. \quad (34)$$

⁸ The expressions for s_L in terms of Λ up to fourth order in perturbation theory may be found in [33] (see, also, Appendix A).

⁹ The FOPT version of this equation reads $\int_0^{s_p} v_1^{\text{FO}}(s) ds = \int_0^{s_p} v_1^{\text{exp}}(s) ds$ (see [3]).

Table 1 The numerical values of the coefficient c_L in the $\overline{\text{MS}}$ scheme as calculated from formula (31) in the case of the four-loop order β -function.

	Approximations to the Adler function				
	LO	NLO	N ² LO	N ³ LO	N ⁴ LO
c_L	0.301262	0.453421	0.555401	0.651373	0.721687

The coefficient c_L is calculated numerically from formula (31). In this calculations we use the exact (explicit) two-loop running coupling and exact (numeric) four-loop running coupling¹⁰. In particular, using the next-to-next-to-leading order approximation (N²LO) to the Adler function constructed in terms of the exact two-loop order running coupling we find

$$c_L|_{\text{two-loop beta}} = 0.421163. \quad (35)$$

The numerical values of the coefficient c_L evaluated in the $\overline{\text{MS}}$ scheme in the case of the four-loop order exact (numeric) running coupling are listed in Table 1. In the calculations we have used the approximations to the Adler function of increasing order¹¹. For the unknown $\mathcal{O}(\alpha_s^5)$ correction to the Adler function, we employ the geometric estimate $d_5 = d_4(d_4/d_3) = 378$ [12].

It follows from the mixed representation (4) for the spectral function that one may calculate in perturbation theory the decay rate of the τ lepton into hadrons of invariant mass larger than $\sqrt{s_p}$

$$R_{\tau,V}^{\text{pert.}}|_{s>s_p} = 6|V_{ud}|^2 S_{EW} \int_{s_p}^{m_\tau^2} w_\tau(s) v_1^{\text{APT}}(s) ds, \quad (36)$$

where

$$w_\tau(s) = \frac{1}{m_\tau^2} \left(1 - \frac{s}{m_\tau^2}\right)^2 \left(1 + 2\frac{s}{m_\tau^2}\right),$$

V_{ud} and S_{EW} denote the flavor mixing matrix element and an electro-weak correction term respectively [6]. Equation (36) reduces to

$$\int_{s_p}^{m_\tau^2} w_\tau(s) v_1^{\text{APT}}(s) ds = \int_{s_p}^{m_\tau^2} w_\tau(s) v_1^{\text{exp}}(s) ds. \quad (37)$$

Using relation (22), we express the left hand side of (37) in terms of the effective spectral density. By integrating by parts, after some algebra, we obtain

$$\begin{aligned} \int_{s_p}^{m_\tau^2} w_\tau(s) v_1^{\text{APT}}(s) ds &= \frac{1}{4} \left(1 - \frac{s_p}{m_\tau^2}\right)^3 \left(1 + \frac{s_p}{m_\tau^2}\right) (1 + r(s_p)) \\ &\quad - \frac{1}{4\pi} \int_{s_p}^{m_\tau^2} \frac{\rho_{\text{eff}}(s)}{s} \left(1 - \frac{s}{m_\tau^2}\right)^3 \left(1 + \frac{s}{m_\tau^2}\right) ds. \end{aligned} \quad (38)$$

To clarify the difference between the APT and APT⁺ frameworks, a few comments are in order: i) In APT the spectral function is determined through formula (22) in

¹⁰ Application of the explicit series solution (13) for the four-loop coupling yield the same results.

¹¹ we will use the abbreviation N^kLO to denote the order $\mathcal{O}(\alpha_s^{k+1})$ approximation to the Adler function.

the entire region $0 < s < \infty$, whereas in APT^+ this formula holds only for $s > s_p$. ii) In APT the RG improved approximation to the Adler function, $D_{\text{RGI}}(Q^2)$, is replaced with corresponding “analytic” image $D_{\text{APT}}(Q^2)$ from the outset. Then formula (28), the definition of the power suppressed contributions to the Adler function must be suitably modified (see [47]). In this paper, we do not mention this procedure. iii) To parametrize our results we use the standard coupling constant $\alpha_s(m_\tau^2)$, whereas in APT the results are parametrized in terms of the analytic coupling $\alpha_s(m_\tau^2)_{\text{an}}$.

3 Numerical Results for the Parameters

To extract the parameters s_p and Λ from the data we have to solve the system of equations

$$\Phi_1(s_p, \Lambda^2) = \int_0^{s_p} v_1^{\text{exp}}(s) ds, \quad (39)$$

$$\Phi_2(s_p, \Lambda^2) = \int_{s_p}^{m_\tau^2} w_\tau(s) v_1^{\text{exp}}(s) ds, \quad (40)$$

where the functions $\Phi_{1,2}$ are defined as

$$\Phi_1(s_p, \Lambda^2) = \frac{s_p}{2}(1 + r(s_p)) + \frac{1}{2\pi} \int_0^{s_p} \rho_{\text{eff}}(\sigma) d\sigma + \frac{c_L}{2} \Lambda^2, \quad (41)$$

$$\begin{aligned} \Phi_2(s_p, \Lambda^2) = & (1 - \hat{s}_p)^3 (1 + \hat{s}_p) \frac{(1 + r(s_p))}{4} \\ & - \frac{1}{4\pi} \int_{\hat{s}_p}^1 \frac{\rho_{\text{eff}}(m_\tau^2 y)}{y} (1 - y)^3 (1 + y) dy, \end{aligned} \quad (42)$$

with $\hat{s}_p = s_p/m_\tau^2$. The right hand sides of Eqs. (39)-(40) are determined in terms of the empirical function $v_1^{\text{exp}}(s)$. We reconstruct the experimental vector spectral function from the ALEPH 2005 spectral data for the vector invariant mass squared distribution which is publicly available [10] (see Appendix B). The spectral function is measured at discrete points of the energy squared. To interpolate the spectral function between these points we use cubic splines.

We solve the system of equations (39)-(40) numerically using various approximations to the Adler function. Since the system is transcendental it has more than one solution. In Table 2, we present the first reasonable solution for the parameters obtained at next-to-next-to-leading order (N²LO). From the Table, we see that the predictions for s_p are stable with respect to the loop corrections to the β -function. In this regard, the predictions for the QCD scale parameter is more sensitive. The two values of Λ obtained with the two- and four-loop β -functions differ in about 10%. However, this corresponds to the small difference $\alpha_s(m_\tau^2)|_{\text{four-loop}} - \alpha_s(m_\tau^2)|_{\text{two-loop}} \approx 0.0017$.

The solution for s_p obtained with the two-loop running coupling should be compared with the estimate $s_p = 1.60 \pm 0.17$ extracted in [3] from the earlier ALEPH data. Our prediction for the central value of s_p (see Table 2) is greater in about 7%. However, with the more accurate data, we have obtained smaller experimental errors on the parameters (see Appendix B). Our estimate for the central value, $\Lambda|_{\{\text{two-loop } \beta\}} = 383 \text{ MeV}$ is somewhat above the value $\Lambda|_{\{\text{two-loop } \beta\}} = 372 \text{ MeV}$

Table 2 The first solution for the parameters s_p and $\Lambda = \Lambda_{\overline{\text{MS}}}$ obtained at N²LO. The two- and four-loop running couplings have been used. The extracted values of the strong coupling constant $\alpha_s(m_\tau^2)$ are also given. The error bars refer to the experimental uncertainty only.

Observable	Approximation to the β -function	
	Two-loop	Four-loop
$s_p \text{ GeV}^2$	1.711 ± 0.054	1.709 ± 0.054
$\Lambda \text{ GeV}$	0.383 ± 0.034	0.348 ± 0.030
$\alpha_s(m_\tau^2)$	0.320 ± 0.015	0.321 ± 0.016

Table 3 The same as in Table 2 for the case of the second solution for the parameters.

Observable	Approximation to the β -function	
	Two-loop	Four-loop
$s_p \text{ GeV}^2$	0.606 ± 0.003	0.607 ± 0.003
$\Lambda \text{ GeV}$	0.583 ± 0.018	0.522 ± 0.016
$\alpha_s(m_\tau^2)$	0.417 ± 0.010	0.424 ± 0.011

Table 4 Numerical values for the parameters in the $\overline{\text{MS}}$ scheme extracted from the τ data order-by-order within the modified procedure based on APT⁺.

Observable	Approximation to the Adler function				
	LO	NLO	N ² LO	N ³ LO	N ⁴ LO
$s_p \text{ GeV}^2$	1.707	1.710	1.709	1.707	1.705
$\Lambda \text{ GeV}$	0.486	0.378	0.348	0.332	0.323
$\alpha_s(m_\tau^2)$	0.401	0.337	0.321	0.313	0.308

accepted in [3]. However, one should keep in mind that in [3] only one equation, the FOPT counterpart of Eq. (39), has been utilized.

Note that the system (39)-(40) permits one more solution for the parameters in the range $200 \text{ MeV} < \Lambda < 600 \text{ MeV}$ (see Table 3). An attractive feature of this solution is that it predicts a smaller value for the onset of perturbation theory: $s_p = 0.607 \text{ GeV}^2 \approx m_\rho^2$ (m_ρ stands for the ρ -meson mass). However, considering current status of α_s we find the extracted value for the strong coupling constant too large. For this reason, we decline this solution.

We also determine the experimental uncertainties on the parameters coming from the uncertainties of the vector invariant mass squared distribution. The correlations between the errors of the distribution are properly taken into account. Cumbersome technical details of the error analysis are relegated into Appendix B.

It is useful to determine the so-called indicative estimates of the theoretical uncertainties on the numerical values of the parameters (for the definition see [27]). This requires us to test convergence of the numerical results order-by order in perturbation theory. We use consecutive approximations to the Adler function from LO to N⁴LO. For the unknown $\mathcal{O}(\alpha_s^5)$ correction, we use the geometric estimate $d_5 = d_4(d_4/d_3) = 378 \pm 378$ [12]. The results for the extracted values of the parameters are presented in Table 4. Formally, we may write a series for the numerical value of the coupling

constant as follows

$$\alpha_s(m_\tau^2)|_{\text{N}^4\text{LO}} = \alpha_s(m_\tau^2)|_{\text{LO}} + \sum_{k=1}^4 \Delta_k,$$

where $\Delta_k = \alpha_s(m_\tau^2)|_{\text{N}^k\text{LO}} - \alpha_s(m_\tau^2)|_{\text{N}^{k-1}\text{LO}}$. Using the numbers listed in Table 4 (we use abbreviation APT^+ for the modified APT accepted in this paper) we obtain the series

$$\alpha_s(m_\tau^2)|_{\text{N}^4\text{LO}}^{\text{APT}^+} = 0.401 - 0.064 - 0.016 - 0.009 - 0.005. \quad (43)$$

The changes of the leading term induced by the consecutive corrections in the series are found to be: 15.9%, 4.0%, 2.2% and 1.2%. It is interesting to compare the series (43) with its counterpart obtained within standard CIPT. Using the standard CIPT to analyze the same data (for details see Appendix C) we obtain the series

$$\alpha_s(m_\tau^2)|_{\text{N}^4\text{LO}}^{\text{CIPT}} = 0.485 - 0.095 - 0.023 - 0.013 - 0.007. \quad (44)$$

We see that within CIPT the corrections provide slightly larger changes of the leading term: 19.6%, 4.7%, 2.7% and 1.4%. One finds that $\Delta_k(\text{CIPT})/\Delta_k(\text{APT}^+) \approx 1.2$ for $k = 1 - 4$. So that the series (43) converges slightly rapidly than the series (44). The indicative estimate of the theoretical uncertainty is determined as a half of the last retained term in the series [27]¹². As pointed out in [27], the error defined in this way is heuristic and indicative. The actual values of the theoretical errors related to the uncalculated higher order terms in the perturbation theory series for the decay rate might be even larger (see, for example, papers [6, 27, 28, 53]). In this paper, however, we shall consider only the indicative theoretical errors. From the series (43), we obtain the estimates

$$\begin{aligned} \alpha_s(m_\tau^2)|_{\text{NLO}} &= 0.337 \pm 0.016_{\text{exp}} \pm 0.032_{\text{th}} \\ \alpha_s(m_\tau^2)|_{\text{N}^2\text{LO}} &= 0.321 \pm 0.016_{\text{exp}} \pm 0.008_{\text{th}} \\ \alpha_s(m_\tau^2)|_{\text{N}^3\text{LO}} &= 0.313 \pm 0.014_{\text{exp}} \pm 0.004_{\text{th}} \\ \alpha_s(m_\tau^2)|_{\text{N}^4\text{LO}} &= 0.308 \pm 0.014_{\text{exp}} \pm 0.002_{\text{th}}, \end{aligned} \quad (45)$$

here we have also included the experimental errors. Analogically, from the CIPT series (44), one obtains

$$\begin{aligned} \alpha_s(m_\tau^2)|_{\text{NLO}} &= 0.390 \pm 0.011_{\text{exp}} \pm 0.048_{\text{th}} \\ \alpha_s(m_\tau^2)|_{\text{N}^2\text{LO}} &= 0.367 \pm 0.009_{\text{exp}} \pm 0.012_{\text{th}} \\ \alpha_s(m_\tau^2)|_{\text{N}^3\text{LO}} &= 0.354 \pm 0.008_{\text{exp}} \pm 0.007_{\text{th}} \\ \alpha_s(m_\tau^2)|_{\text{N}^4\text{LO}} &= 0.347 \pm 0.008_{\text{exp}} \pm 0.003_{\text{th}}, \end{aligned} \quad (46)$$

The N^4LO estimates in (45) and (46) correspond to the central value $d_5 = 378$. The additional theoretical error in the coupling constant induced from the uncertainty in the fifth order unknown coefficient ($d_5 = 378 \pm 378$) takes the values 0.0045 ($\approx 1.5\%$) and 0.0065 ($\approx 1.9\%$) in the new and standard extraction procedures respectively¹³. Comparing the numbers in formulas (45) and (46), we see that the indicative estimates of the theoretical error are smaller within the new procedure. In contrast to this, the experimental errors on the values of α_s increases by the factor of 1.76 within the

¹² In [27] this definition of the uncertainty has been used within FOPT.

¹³ With $d_5 = 756$, we have obtained $\alpha_s(m_\tau^2)|_{\text{APT}^+} = 0.3035$ and $\alpha_s(m_\tau^2)|_{\text{CIPT}} = 0.3407$.

new procedure. It is remarkable that a more reliable estimate of the theoretical error presented in [12] is close to the $N^3\text{LO}$ and $N^4\text{LO}$ values of the indicative error given in formula (46).

Similarly, determining the indicative theoretical errors on the parameter s_p , we find the stable results

$$\begin{aligned} s_p|_{\text{NLO}} &= 1.710 \pm 0.054_{\text{exp}} \pm 0.002_{\text{th}} \quad \text{GeV}^2 \\ s_p|_{\text{N}^2\text{LO}} &= 1.709 \pm 0.054_{\text{exp}} \pm 0.001_{\text{th}} \quad \text{GeV}^2 \\ s_p|_{\text{N}^3\text{LO}} &= 1.707 \pm 0.054_{\text{exp}} \pm 0.001_{\text{th}} \quad \text{GeV}^2 \\ s_p|_{\text{N}^4\text{LO}} &= 1.705 \pm 0.054_{\text{exp}} \pm 0.001_{\text{th}} \quad \text{GeV}^2. \end{aligned} \quad (47)$$

Notice that the ratio $\alpha_s(s_p)/\alpha_s(m_\tau^2) \approx 1.22$ is not large. However, the APT^+ expansion formally depends on the small energy scale $\sqrt{s_p} \approx 1.31\text{GeV}$. So, it is reasonable to justify the applicability of the perturbation theory in the APT^+ framework. The issue of the applicability of perturbation theory in τ decays has been previously addressed in [63]. It was pointed out [63] that this question is phenomenological one, and it cannot be answered yet from theoretical grounds. In particular, the decay rate of the τ lepton into hadrons of invariant mass squared smaller than s_0 ($s_0 < m_\tau^2$) has been analyzed within FOPT. Using the ALEPH spectral data, the authors of [63] have deduced that the rate can be calculated in pQCD with high accuracy for $s_0 > s_{\text{min.}} = 0.7\text{GeV}^2$. Note that our estimate for s_p clearly satisfies this condition, $s_p/s_{\text{min.}} \approx 2.4$. Nevertheless, it is desirable to investigate numerically the convergence of the perturbative expansion within APT^+ . Let us derive the expansion for the τ -lepton decay rate from formula (36). The integral on the right of (36) can be approximated by a non-power series. To derive the non-power series, we express the spectral function in terms of the effective spectral density using formulas (22) and (23). Then we expand the function $\rho_{\text{eff}}(s)$ in perturbation theory using formulas (14) and (18). So, we obtain

$$\hat{R}_{\tau,V}^{\text{pert.}}|_{s>s_p} = R_{\tau,V}^{\text{pert.}}|_{s>s_p}/\{6|V_{\text{ud}}|S_{\text{EW}}\} = \sum_{k=0}^5 d_k \mathfrak{A}_k(m_\tau^2, s_p) \quad (48)$$

where

$$\mathfrak{A}_0(m_\tau^2, s_p) = f(s_p/m_\tau^2), \quad (49)$$

$$\mathfrak{A}_{k \geq 1}(m_\tau^2, s_p) = r_k(s_p)f(s_p/m_\tau^2) - \frac{1}{\pi} \int_{s_p}^{m_\tau^2} \frac{f(\sigma/m_\tau^2)}{\sigma} \rho_k(\sigma) d\sigma, \quad (50)$$

here we have used the notations: $f(x) = \frac{1}{4}(1-x)^3(1+x)$ and

$$\begin{aligned} \rho_k(\sigma) &= \text{Im}\{a_s^k(-\sigma - i0)\}, \\ r_k(s_p) &= \frac{1}{\pi} \int_{s_p}^{\infty} \frac{\rho_k(\sigma)}{\sigma} d\sigma. \end{aligned} \quad (51)$$

The first term in the series (48), \mathfrak{A}_0 , corresponds to the (modified) parton level contribution to the rate. We calculate the functions \mathfrak{A}_k numerically by using analytic expressions for the functions $\rho_k(\sigma)$ (see formula (63) in Appendix A). In the calculation, we employ the four-loop running coupling. For the parameters s_p and $\Lambda \equiv \Lambda_{\overline{\text{MS}}}$, we use the numerical values from the Table 4, namely, the values extracted from the ALEPH

Table 5 Comparison of the expansion functions $\mathfrak{A}_k(m_\tau^2, s_p)$, $\mathcal{A}_k(m_\tau^2)$ and the powers of the “couplant” $a_s(m_\tau^2)$. The four-loop “couplant” is calculated using the value $\Lambda = 0.3225$ GeV. To calculate the functions $\mathfrak{A}_k(m_\tau^2, s_p)$, we have used the values $\Lambda|_{\text{N}^4\text{LO}} = 0.3225$ GeV and $s_p|_{\text{N}^4\text{LO}} = 1.7053$ GeV obtained within APT⁺. To calculate the functions $\mathcal{A}_k(m_\tau^2)$ we have used the value $\Lambda|_{\text{N}^4\text{LO}} = 0.395$ GeV obtained from the ALEPH data within CIPT.

k	$a_s^k(m_\tau^2)$	$\mathcal{A}_k(m_\tau^2)$	$\mathfrak{A}_k(m_\tau^2, s_p)$
1	$0.9797 \cdot 10^{-1}$	0.1511	$0.3275 \cdot 10^{-2}$
2	$0.9599 \cdot 10^{-2}$	$0.1876 \cdot 10^{-1}$	$0.2400 \cdot 10^{-3}$
3	$0.9405 \cdot 10^{-3}$	$0.2000 \cdot 10^{-2}$	$0.1455 \cdot 10^{-4}$
4	$0.9214 \cdot 10^{-4}$	$0.1834 \cdot 10^{-3}$	$0.6733 \cdot 10^{-6}$
5	$0.9028 \cdot 10^{-5}$	$0.1383 \cdot 10^{-4}$	$0.1599 \cdot 10^{-7}$

data within APT⁺ at N⁴LO. Using analytically known coefficients d_k , $k = 0 - 4$ and the estimate $d_5 = 378$, we obtain from Eq. (48) the expansion

$$\hat{R}_{\tau,V}^{\text{pert.}}|_{s>s_p} = 0.3747 \cdot 10^{-1} + 0.3275 \cdot 10^{-2} + 0.3937 \cdot 10^{-3} + 0.9270 \cdot 10^{-4} + 0.3304 \cdot 10^{-4} + (0.6047 \cdot 10^{-5}) \approx 0.04127. \quad (52)$$

Consider now the non-power expansion for the perturbation theory correction $\delta^{(0)}$ obtained within CIPT [24] (see Appendix C)

$$\delta_{\text{CI}}^{(0)} = \sum_{k=1} d_k \mathcal{A}_k(m_\tau^2), \quad (53)$$

where

$$\mathcal{A}_k(m_\tau^2) = \frac{1}{\pi} \int_0^\pi \text{Re}\{(1 - e^{i\phi})(1 + e^{i\phi})^3 a_s^k(m_\tau^2 e^{i\phi})\} d\phi,$$

to calculate these functions numerically, we employ for the scale parameter Λ the numerical value extracted from the ALEPH data within CIPT at N⁴LO (see Table 14). At N⁴LO, the expansion (53) can be rewritten as

$$\delta_{\text{CI}}^{(0)} = 0.1513 + 0.3081 \cdot 10^{-1} + 0.1276 \cdot 10^{-1} + 0.9012 \cdot 10^{-2} + (0.5233 \cdot 10^{-2}) \approx 0.2091. \quad (54)$$

Comparing the numerical expansions in Eqs. (52) and (54), one sees that the APT⁺ series (52) displays a faster convergence. In the CIPT expansion (54), the corrections provide a 38% change of the leading term. In contrast, in the APT⁺ expansion (52) the corrections provide only a 16% change of the leading term (we recall that the leading QCD correction in (52) is the second term in the series).

The rapid convergence of the series (52) may be explained due to the specific properties of the expansion functions $\mathfrak{A}_k(m_\tau^2, s_p)$. The set of functions $\{\mathfrak{A}_k(m_\tau^2, s_p)\}$ can be viewed as a generalization of the analogical set of functions considered in the Shirkov-Solovtsov APT (for properties of the APT expansion functions see [42]). In Table 5, we have compared functions $\mathfrak{A}_k(m_\tau^2, s_p)$ with the functions $\mathcal{A}_k(m_\tau^2)$. For the sake of comparison, we also include in the Table the powers of the “couplant” $a_s(m_\tau^2)$. It is seen from the Table that the functions $\mathfrak{A}_k(m_\tau^2, s_p)$ decrease with k much more rapidly than the functions $\mathcal{A}_k(m_\tau^2)$ and $a_s^k(m_\tau^2)$.

Usually, it is convenient to perform evolution of the α_s results to the reference scale $M_z = 91.187$ GeV. This is done by using RG equation and appropriate matching conditions at the heavy quark (charm and bottom) thresholds (see [64] and literature

Table 6 Estimates for $\alpha_s(M_z^2)$ obtained from the ALEPH τ lepton decay vector data order-by-order in perturbation theory. The results obtained within APT⁺ and CIPT are compared. Two errors are given, the experimental (first number) and the error from the evolution procedure (second number).

Perturbative order	$\alpha_s(M_z^2) _{\text{APT}^+}$	$\alpha_s(M_z^2) _{\text{CIPT}}$
N ² LO	$0.1187 \pm 0.0019 \pm 0.0005$	$0.1238 \pm 0.0009 \pm 0.0005$
N ³ LO	$0.1176 \pm 0.0018 \pm 0.0005$	$0.1224 \pm 0.0009 \pm 0.0005$
N ⁴ LO	$0.1170 \pm 0.0018 \pm 0.0005$	$0.1217 \pm 0.0009 \pm 0.0005$

Table 7 Comparison of the RSI and APT⁺ determinations of the $\overline{\text{MS}}$ coupling constant from the τ -decay data. Experimental errors are given only.

Perturbative order	$\alpha_s(m_\tau^2) _{V+A}^{\text{RSI}}$	$\alpha_s(m_\tau^2) _V^{\text{APT}^+}$
NLO	0.278 ± 0.003	0.335 ± 0.016
N ² LO	0.319 ± 0.004	0.321 ± 0.016
N ³ LO	0.312 ± 0.004	0.313 ± 0.014

therein). The three-loop level matching conditions in the $\overline{\text{MS}}$ scheme were derived in [65]. In this paper, we follow the work [66], where a very accurate analytic approximation to the four-loop running coupling was suggested. We perform the matching at the matching scale $m_{\text{th}} = 2\mu_h$ where μ_h is a scale invariant $\overline{\text{MS}}$ mass of the heavy quark $\mu_h = \overline{m}_h(\mu_h)$. We assume for the scale invariant $\overline{\text{MS}}$ masses the values $\mu_c = 1.27_{-0.11}^{+0.07}$ GeV and $\mu_b = 4.20_{-0.07}^{+0.17}$ GeV [67]. Following [66], we evaluate the central value and error of $\alpha_s(M_z^2)$ according to the formulas

$$\alpha_s(M_z^2) = (\alpha_s^+(M_z^2) + \alpha_s^-(M_z^2))/2 \quad \text{and} \quad \Delta\alpha_s(M_z^2) = (\alpha_s^+(M_z^2) - \alpha_s^-(M_z^2))/2$$

where $\alpha_s^\pm(M_z^2)$ denote the values obtained from $\alpha_s^\pm(m_\tau^2) = \alpha_s(m_\tau^2) \pm \Delta\alpha_s(m_\tau^2)$. In the evolution procedure, we have used the exact numeric four-loop running coupling¹⁴. In Table 6, we compare the estimates for $\alpha_s(M_z^2)$ obtained within the new (APT⁺) and standard (CIPT) procedures.

Finally, for the sake of comparison, let us extract the numerical values for the coupling constant from τ decay (V+A) data using the renormalization scheme invariant extraction procedure (RSI) of [27]. This procedure is based on FOPT. For the experimental value of the perturbative part of the τ decay rate in the non-strange (V+A) channel, we assume the updated value, presented in [26],

$$\delta_{\text{exp}}^{(0)}|_{V+A} = 0.2042 \pm 0.0050_{\text{exp}}.$$

For consistency reasons we use the $\overline{\text{MS}}$ scheme β -function to the k-loop order with the N^{k-1}LO approximation to the Adler function. In Table (7) we compare numerical values for $\alpha_s(m_\tau^2)$ obtained within the two approaches, RSI and APT⁺. The relevant channels which have been used to extract the coupling are indicated by subscripts. One sees from the Table, that beyond NLO there is a good agreement between the two methods of the $\alpha_s(m_\tau^2)$ determination.

¹⁴ We have confirmed that the approximate analytical coupling derived in [66] leads practically to the same numerical results.

Table 8 Comparison of the “experimental” Adler function $D_{\text{“exp”}}(Q^2)$ with its QCD component $D_{\text{pQCD}}(Q^2, s_p)$ at low momenta. The perturbative component is evaluated within APT^+ at N^2LO using the four-loop running coupling. The absolute and relative statistical errors of the “experimental” Adler function are tabulated.

Q GeV	$D_{\text{“exp”}}(Q^2)$	$D_{\text{pQCD}}(Q^2, s_p)$	$\sigma(D_{\text{“exp”}})$	rel.err.
0.1	0.0649	0.0063	0.0061	9.5%
0.2	0.2300	0.0249	0.0198	8.6%
0.3	0.4354	0.0545	0.0333	7.7%
0.4	0.6320	0.0933	0.0426	6.7%
0.5	0.7944	0.1391	0.0473	6.0%
0.6	0.9162	0.1895	0.0484	5.3%
0.7	1.0016	0.2426	0.0471	4.7%
0.8	1.0583	0.2965	0.0445	4.2%
0.9	1.0942	0.3497	0.0412	3.8%
1.0	1.1157	0.4013	0.0377	3.4%

4 Numerical Results for the “Experimental” Adler Function

Looking at the numbers in Table 2, we see that our estimates for the parameters are somewhat different than those used previously in [3]. Hence, it is sensible to recalculate the experimental Adler function in the infrared region. Another reason to do this is the appearance of the improved τ data [10]. More importantly, it is desirable to carry out the error analysis too. Furthermore, in contrast to [3], in our calculations we will employ APT^+ .

The “experimental” Adler function and its QCD component are tabulated in Table 8. The QCD component of the “experimental” Adler function is calculated numerically at N^2LO from formula (25). In the calculations we employ the four-loop running coupling. For the parameters s_p and Λ , we use the values from Table 2. The absolute ($\pm 1\sigma$) and relative (in percents) experimental errors of the “experimental” Adler function are also tabulated. The error analysis is described in Appendix B. We see from the Table that the pQCD component has sizeable contribution to the total “experimental” Adler function. This contribution increases monotonically with Q from 10% (at $Q = 0.1$ GeV) to 36% (at $Q = 1$ GeV).

To test the stability of the numerical results with regards to the higher order corrections to the β -function, we have compared two results for the “experimental” Adler function that are obtained with the two- and four-loop exact running couplings. The pQCD component of the Adler function has been evaluated within APT^+ at N^2LO . For the parameters s_p and Λ , we have used the central values given in Table 2. In the region $Q = 0 - 1.5$ GeV, the difference between using the two- or four-loop approximation to the β -function is found to be quite small ($\sim 0.05\%$). The approximation corresponding to the two-loop running coupling takes slightly large values.

To test the stability of numerical results with regards to higher order corrections to the Adler function, we use various approximations to the pQCD component (see Table 9). We see from the Table that the differences between the consecutive approximations to the “experimental” Adler function slowly increase as a function of the scale. Already, the leading order approximation provides a very accurate result. At $Q = 1.5$ GeV (where the changes induced by the loop correction take maximal values) the differences between consecutive approximations (i.e. the differences between the

Table 9 Different approximations to the “experimental” Adler function as a function of the scale. The function $D_{\text{“exp”}}^{(k)}(Q^2)$ has the pQCD component evaluated within APT⁺ at N^(k-1)LO. To construct this component, we employ the four-loop order running coupling.

Q GeV	$D_{\text{“exp”}}^{(1)}(Q^2)$	$D_{\text{“exp”}}^{(2)}(Q^2)$	$D_{\text{“exp”}}^{(3)}(Q^2)$	$D_{\text{“exp”}}^{(4)}(Q^2)$	$D_{\text{“exp”}}^{(5)}(Q^2)$
0.1	0.06494	0.06494	0.06494	0.06494	0.06494
0.2	0.23003	0.23005	0.23004	0.23003	0.23002
0.3	0.43541	0.43546	0.43544	0.43541	0.43539
0.4	0.63196	0.63205	0.63201	0.63196	0.63192
0.5	0.79431	0.79444	0.79438	0.79430	0.79424
0.6	0.91613	0.91631	0.91623	0.91612	0.91604
0.7	1.0015	1.0017	1.0016	1.0015	1.0014
0.8	1.0582	1.0585	1.0583	1.0582	1.0580
0.9	1.0940	1.0943	1.0942	1.0940	1.0938
1.0	1.1154	1.1158	1.1157	1.1154	1.1152
1.5	1.1321	1.1327	1.1324	1.1320	1.1317

N^{k-1}LO and N^kLO approximations) take the values 0.05%, 0.03%, 0.03% and 0.03% for $k = 1, 2, 3$ and 4 respectively.

It is instructive to investigate numerically the convergence property of the non-power series for the perturbation theory component $D_{\text{pQCD}}(Q^2, s_p)$. The non-power series is obtained from formula (25) by using perturbation theory expansions for the function $\rho_{\text{eff}}(s)$ and $r(s)$ (see formulas (14), (18) and (23)). The non-power series read

$$D_{\text{pQCD}}(Q^2, s_p) = \sum_{k=0} d_k \mathfrak{D}_k(Q^2, s_p), \quad (55)$$

where

$$\mathfrak{D}_0(Q^2, s_p) = \frac{Q^2}{(s_p + Q^2)}, \quad (56)$$

$$\mathfrak{D}_{k \geq 1}(Q^2, s_p) = \frac{Q^2}{(s_p + Q^2)} r_k(s_p) - \frac{Q^2}{\pi} \int_{s_p}^{\infty} \frac{\rho_k(\sigma)}{\sigma(\sigma + Q^2)} d\sigma, \quad (57)$$

the functions $\rho_k(\sigma)$ and $r_k(s_p)$ are defined in Eqs. (51). Let us truncate the non-power expansion (55) at N⁴LO (i.e. for $k = 5$). Using the N⁴LO estimates for the parameters given in Table 4, we evaluate the ratios of the consecutive terms of the series

$$\mathcal{R}_k(Q^2) = (d_k/d_{k-1}) \mathfrak{D}_k(Q^2, s_p) / \mathfrak{D}_{k-1}(Q^2, s_p),$$

for $k = 1 - 5$. In Table 10, we tabulate numerical values of these ratios in the region $Q = 0.1 - 1.5$ GeV. It is seen from the Table, that the magnitudes of the ratios are sufficiently small to guarantee fast numerical convergence of the series: $\mathcal{R}_k(Q^2) \leq 0.368$ ($k = 1 - 5$) for all values of Q in the considered interval.

Let us now compare our numerical results on the “experimental” Adler function with the previous results of work [3]. First, we repeat the calculation within the approach of [3] using the improved data. Assuming the value $\Lambda_{\overline{\text{MS}}} = 372 \pm 76$ MeV used in [3], we solve numerically the FOPT counterpart of the equation (39). Thus we find the solution $s_p = 1.621 \pm 0.163$ GeV². The central value of this estimate is slightly large, by 0.021, than the value obtained in [3]. Using the values $s_p = 1.621$ GeV² and $\Lambda_{\overline{\text{MS}}} = 372$ MeV, we calculate the “experimental” Adler function within the (modified)

Table 10 The ratios of the consecutive terms in the non-power series (55) as a function of the scale.

Q GeV	$\mathcal{R}_1(Q^2)$	$\mathcal{R}_2(Q^2)$	$\mathcal{R}_3(Q^2)$	$\mathcal{R}_4(Q^2)$	$\mathcal{R}_5(Q^2)$
0.1	0.077	0.112	0.228	0.366	0.238
0.3	0.077	0.111	0.228	0.366	0.240
0.5	0.077	0.111	0.227	0.366	0.242
0.7	0.076	0.110	0.226	0.367	0.245
1.0	0.075	0.109	0.225	0.367	0.251
1.3	0.073	0.108	0.223	0.368	0.257
1.5	0.072	0.107	0.222	0.368	0.261

Table 11 Comparison of the “experimental” Adler functions evaluated within the modified FOPT and APT⁺. The pQCD components of the functions are constructed at N²LO with the two-loop order running coupling. The pQCD component of $D(Q^2)|_{\text{“exp”}}^{\text{FOPT}}$ corresponds to the values $\Lambda_{\overline{\text{MS}}} = 372$ MeV and $s_p = 1.621$ GeV². The pQCD component of $D(Q^2)|_{\text{“exp”}}^{\text{APT}^+}$ corresponds to the values $\Lambda_{\overline{\text{MS}}} = 383$ MeV and $s_p = 1.711$ GeV². The relative difference between these functions is also tabulated.

Q GeV	$D(Q^2) _{\text{“exp”}}^{\text{FOPT}}$	$D(Q^2) _{\text{“exp”}}^{\text{APT}^+}$	rel.diff.
0.1	0.0651	0.0649	0.31%
0.2	0.2305	0.2301	0.20%
0.3	0.4364	0.4355	0.21%
0.4	0.6336	0.6321	0.24%
0.5	0.7967	0.7945	0.28%
0.6	0.9191	0.9164	0.29%
0.7	1.0050	1.0018	0.32%
0.8	1.0621	1.0586	0.33%
0.9	1.0982	1.0945	0.34%
1.0	1.1197	1.1160	0.33%
1.1	1.1316	1.1280	0.32%
1.2	1.1371	1.1337	0.30%
1.3	1.1386	1.1355	0.27%
1.4	1.1377	1.1350	0.24%
1.5	1.1354	1.1330	0.21%

FOPT at N²LO. This should be compared with the new approximation computed in the same order within APT⁺. In the case of APT⁺, we use the values $\Lambda_{\overline{\text{MS}}} = 383$ MeV and $s_p = 1.711$ GeV² (see Table 2). To be consistent with [3], we use the two-loop exact running coupling. In Table 11, we compare numerically two approximations to the “experimental” Adler function, the functions $D_{\text{“exp”}}^{\text{FOPT}}(Q^2)$ and $D_{\text{“exp”}}^{\text{APT}^+}(Q^2)$. From the Table, we see that the functions are close, but $D_{\text{“exp”}}^{\text{FOPT}}(Q^2) > D_{\text{“exp”}}^{\text{APT}^+}(Q^2)$. The relative difference between the functions in the considered region varies in the interval 0.20% – 0.34%.

5 Conclusion

We have extracted the numerical values of the strong coupling constant α_s and the parameter s_p (the square of the boundary energy) from the non-strange vector τ data provided by ALEPH. Based on the semi-empirical representation (4) for the hadronic

non-strange vector spectral function, we have developed a modified extraction procedure. This procedure enabled us to avoid direct application of the standard OPE formalism in Minkowski space. The distinguishing feature of our analysis is that we have determined the two parameters (α_s and s_p) simultaneously from the data.

In Sect. 2, we have derived a violated DR for the RG improved perturbation theory correction to the Adler function, the formula (16). Using the violated DR, we have shown that the perturbation theory component of the “experimental” spectral function is determined via the APT formula (22). This determines the hadronic spectral function in terms of the effective spectral density, $\rho_{\text{eff}}(\sigma)$, the basic object of the perturbation theory calculation. We have obtained a convenient expression for the pQCD part of the “experimental” Adler function in terms of the effective spectral density, the formula (25). Using the violated DR (16), we have determined the power suppressed corrections to the “experimental” Adler function via the formula (29). Making further use of the consistency condition from the OPE for the “experimental” Adler function, we have derived Eq. (34). This equation relates the parameters s_p and Λ to the values of the hadronic spectral function on the range $0 < s < s_p$. Next we used the *ansatz* (4) for the spectral function to calculate the τ decay rate $R_{\tau,V}|_{s>s_p}$. In this way, we have derived Eq. (37) which relates the parameters to the integral of the hadronic spectral function (multiplied by known function) over the range $s_p < s < m_\tau^2$.

In Sect. 3, we have solved, numerically, the obtained system of equations for the parameters s_p and $\Lambda \equiv \Lambda_{\overline{\text{MS}}}$. To examine the convergence of the numerical results for the parameters, we have used perturbation theory approximations to the Adler function up to the $N^4\text{LO}$. The indicative estimates of the theoretical errors [27] are used as a criterion of the quality of the approximations. Based on this criterion, we have demonstrated that the new framework (APT^+), compared to the standard one (CIPT), provides a better numerical convergence for the extracted value of the coupling constant $\alpha_s(m_\tau^2)$. It is remarkable that the central values of the coupling constant extracted within APT^+ in different orders of perturbation theory become systematically smaller as compared to the corresponding values obtained within CIPT (cf. formulas (45) and (46)). The changes in the central values are not within the quoted experimental and theoretical errors. At $N^3\text{LO}$ The central values of $\alpha_s(m_\tau^2)$ in formulas (45) and (46) differ from each other in about 2.7 standard deviation, if the error is determined within APT^+ , $\sigma = \sqrt{\sigma_{\text{exp}}^2 + \sigma_{\text{th}}^2} \approx 0.0151$. With the error obtained in CIPT, $\sigma \approx 0.0107$, one finds even large difference, 3.8σ ¹⁵.

We have examined the stability of the numerical value for the duality point s_d with regard to perturbation theory corrections. We have obtained a surprisingly stable result (see formulas (47)) $s_d = 1.71 \pm 0.05_{\text{exp}} \pm 0.00_{\text{th}}$. GeV^2 . Our prediction for the central value of this parameter is higher in about 7% than the value presented previously in [3].

Having included into analysis the fourth order coefficient d_4 , we achieved excellent agreement between the lattice and tau-decay determinations of the strong coupling constant (at $N^4\text{LO}$ the central value of the constant given in Table (6) coincides with the central value quoted in (2)). For this reason we believe that APT^+ provides better approximation than CIPT.

To justify the applicability of APT^+ in calculations of the τ -lepton decay rates, we examine numerically the APT^+ series. The APT^+ expansion for the rate $R_{\tau,V}|_{s>s_p}$ represents asymptotic expansion over a non-power set of specific functions $\{\mathfrak{A}_n(m_\tau, s_p)\}$

¹⁵ Due to the larger experimental error obtained within APT^+ , $\sigma_{\text{APT}}/\sigma_{\text{CIPT}} \approx 1.4$.

rather than the powers of $a_s(m_\tau^2)$. The APT^+ and CIPT series for the rates $R_{\tau,V}|_{s>s_p}$ and $R_{\tau,V}$ have been compared numerically. We have confirmed that the APT^+ expansion displays a faster convergence.

Our approach confirms that there is a theoretical systematic uncertainty not included in the error assessments obtained in previous studies by ignoring the higher order OPE contributions, the conclusion achieved in work [14]. In this connection, our study suggests that the truncated OPE series cannot approximate sufficiently accurately the integrals of the spectral function over the low energy region $0 < s < s_p \sim 1.7 \text{ GeV}^2$.

In Sect. 4, we have recalculated the “experimental” Adler function within the APT^+ prescription using the new estimates for the parameters s_p and Λ . In addition, we have determined the errors on this function coming from the uncertainties of the parameters and spectral function. Numerical results for the Adler function obtained within APT^+ have been found to be remarkable stable in perturbation theory (see Tables 9 and 10).

In Appendix A, we have given practical formulas for numerical calculation of the $\overline{\text{MS}}$ running coupling at higher orders. The Lambert-W solutions to the RG equation is reviewed. An accurate analytic approximation to the effective spectral density $\rho_{\text{eff}}(\sigma)$ at higher orders is derived. In Appendix B, we have derived formulas (within APT^+) for calculating the experimental uncertainties on the extracted values of the parameters and on the “experimental” Adler function. In Appendix C, we have analyzed the ALEPH non-strange vector spectral data within the standard CIPT prescription. Namely, we have performed some necessary calculations needed for comparing the CIPT and APT^+ prescriptions (see Sect. 3).

The procedure suggested here can be obviously extended to analyze the non-strange τ -data from the axial-vector (A) and vector plus axial-vector (V+A) channels. To check the reliability of the new extraction procedure, it is desirable to compare the V, A, and V+A determinations of the coupling constant. A similar framework may be constructed on the basis of FOPT. This will enable us to estimate total theoretical errors on the extracted values of the parameters Λ and s_p . It should be remarked that a shortcoming of the ansatz (4) is that it completely ignores the non-perturbative contributions to the spectral function coming from the region $s > s_p$. The importance of these contributions for accurate determination of the coupling constant has been demonstrated in recent studies [20,21]. We hope to report on these aspects in future publications.

Acknowledgements I am very grateful for the support of my colleagues at Department of Theoretical Physics at Andrea Razmadze Mathematical Institute. I wish to thank S. Peris and Z. Zhang for helpful correspondence and discussions regarding experimental aspects of spectral function determinations. I thank the referees for valuable comments and corrections. The present work has been partially supported by the Georgian National Science Foundation under grants No GNSF/ST08/4-405 and No GNSF/ST08/4-400.

A A Series Solution to the Renormalization Group Equation

In our notation the RG equation for the running coupling reads

$$\frac{d}{d \ln Q^2} a_s = \beta(a_s) = -a_s^2 \sum_{n=0} \beta_n a_s^n, \quad (58)$$

where $a_s \equiv a_s(Q^2) = \alpha_s(Q^2)/\pi$ with $\alpha_s(Q^2)$ being the running coupling. In the $\overline{\text{MS}}$ scheme, the β -function coefficients are known to four loops [69]. For three active quark flavours the

first four coefficients take the values

$$\beta_0 = 9/4, \quad \beta_1 = 4, \quad \beta_2 = 10.05990, \quad \beta_3 = 47.22804.$$

In general, the RG equation (58), to an arbitrary order in perturbation theory, can not be solved explicitly for the coupling. Usually, the equation is solved in the asymptotical regime $\frac{Q^2}{\Lambda^2} \gg 1$. For our purposes the asymptotic solution is not suitable, since we need an accurate solution at relatively low energies. One may, of course, solve the RG equation numerically. However, it is more convenient to derive some accurate analytic approximation to the coupling. Fortunately, it is possible to solve the RG equation explicitly for the coupling at the two-loop order [30, 31]. The explicit expression for the $\overline{\text{MS}}$ scheme running coupling at the two-loop order reads

$$a_s^{(2)}(Q^2) = -\frac{\beta_0}{\beta_1} \frac{1}{1 + W_{-1}(\zeta)} : \quad \zeta = -\frac{1}{eb_1} \left(\frac{Q^2}{\Lambda^2} \right)^{-1/b_1}, \quad (59)$$

where β_0 and β_1 are the first two β -function coefficients

$$\beta_0 = \frac{1}{4} \left(11 - \frac{2}{3} n_f \right), \quad \beta_1 = \frac{1}{16} \left(102 - \frac{38}{3} n_f \right),$$

$b_1 = \beta_1/\beta_0^2$, $\Lambda \equiv \Lambda_{\overline{\text{MS}}}$ and W_{-1} denotes the branch of the Lambert W function [70].

The coupling to higher orders may be expanded in powers of the two-loop order coupling [61, 62]

$$a_s^{(k>2)}(Q^2) = \sum_{n=1}^{\infty} c_n^{(k)} a_s^{(2)n}(Q^2), \quad (60)$$

The first two coefficients in this series are universal: $c_1^{(k)} = 1$ and $c_2^{(k)} = 0$ (the condition $c_2^{(k)} = 0$ follows from the conventional definition of the Λ parameter). Other coefficients are determined in terms of the β -function coefficients. The four-loop expressions for the first several coefficients are given by

$$c_3^{(4)} = \frac{\beta_2}{\beta_0}, \quad c_4^{(4)} = \frac{\beta_3}{2\beta_0}, \quad c_5^{(4)} = \frac{5}{3} \left(\frac{\beta_2}{\beta_0} \right)^2 - \frac{\beta_1\beta_3}{6\beta_0^2}, \dots$$

It was proved in [33] that the series has a finite radius of convergence, and the radius is sufficiently large for all n_f values of practical interest. Partial sums of the series (60) provide very accurate approximations to the higher order coupling in the wide range of Q^2 . In particular, these approximations may be safely used at low energies. Thus, for $Q = 1$ GeV and $\Lambda = 0.347$ GeV, the partial sum with the first twelve terms reproduce the exact four-loop coupling with the precision better than 0.02%. Using the exact solution (59), the analytical structure of the two-loop coupling in the complex Q^2 -plane has been determined [30, 31]. It was found that the coupling is an analytic function in the whole complex plane except the cuts running along the real Q^2 axis. Besides the physical cut $\{Q^2 : -\infty < Q^2 < 0\}$ corresponding to the logarithmic singularity at $Q^2 = 0$, there is also the ‘‘Landau’’ cut $\{Q^2 : 0 < Q^2 < Q_L^2\}$ corresponding to the Landau singularity on the positive Q^2 -axis. The Landau singularity is a second order algebraic branch point located at $Q_L^2 = b_1^{-b_1} \Lambda^2$ ($b_1^{-b_1} \approx 1.205$ for $n_f = 3$). The relevant branch of the Lambert function on the complex Q^2 plane is determined by the analytical continuation. For the physical vales of n_f ($0 < n_f \leq 6$) the relevant branch is W_{-1} on the upper-half plane, whereas the branch is W_1 on the lower-half plane. A limiting value of the coupling from above the physical cut ($Q^2 = -\sigma + i0$, $\sigma > 0$) is then determined by [32]

$$a_s^{(2)}(-\sigma + i0) = -\frac{\beta_0}{\beta_1} \frac{1}{1 + W_{-1}(\zeta_+)} \quad \text{with} \quad \zeta_+ = \frac{1}{eb_1} \left(\frac{\sigma}{\Lambda^2} \right)^{-1/b_1} \exp \left\{ -i\pi \left(\frac{1}{b_1} - 1 \right) \right\}, \quad (61)$$

similarly, one may write

$$a_s^{(2)}(-\sigma - i0) = -\frac{\beta_0}{\beta_1} \frac{1}{1 + W_1(\zeta_-)} \quad \text{with} \quad \zeta_- = \frac{1}{eb_1} \left(\frac{\sigma}{\Lambda^2} \right)^{-1/b_1} \exp \left\{ i\pi \left(\frac{1}{b_1} - 1 \right) \right\}. \quad (62)$$

Table 12 Numerical values of the first twelve coefficients in the expansion (60) for the four-loop running coupling at $n_f = 3$ quark flavours.

n	c_n		n	c_n
1	1		7	392.1241
2	0		8	2413.463
3	3863/864		9	8248.857
4	10.49512		10	31348.18
5	27.09804		11	147697.8
6	190.2642		12	507565.0

Note that the limiting values $a_s^{(2)}(-\sigma \pm i0)$ satisfy the Schwarz ‘principle of reflection’,

$a_s^{(2)}(-\sigma - i0) = \overline{a_s^{(2)}(-\sigma + i0)}$, provided that W has *near conjugate* symmetry [70]:

$$W_k(\bar{z}) = W_{-k}(z).$$

We may construct an analytic approximation to the Adler function in perturbation theory using formula (60) for the four-loop running coupling. In this approximation, the Adler function is an analytic function in the cut complex Q^2 plane. It has the branch points at $Q^2 = 0$ and $Q^2 = Q_L^2 = b_1^{-b_1} \Lambda^2 > 0$. The effective spectral density (18) associated with the Adler function is then readily calculated, leading to the analytic expression

$$\rho_{\text{eff}}(\sigma) = \text{Im} \left\{ \sum_{n=1}^N d_n \left(\sum_{m=1}^N c_m^{(4)} a_s^{(2)m} (-\sigma - i0) \right)^n \right\}, \quad (63)$$

where $N \geq 3$ and $a_s^{(2)}(-\sigma - i0)$ is determined in terms of the W function as given in formula (62). Formula (63) considerably simplifies numerical calculations of integrals of the effective spectral function (computer algebra system Maple has an arbitrary precision implementation of all branches of the Lambert function). In the most of the calculations, we have used the truncated series (60) for the four-loop running coupling preserving the first twelve terms in the series. Numerical values of the first twelve coefficients of the series, for $n_f = 3$ quark flavours, are tabulated in Table 12.

B The Error Analysis

In this appendix we will evaluate the experimental errors on the extracted values of the parameters. We will also determine the errors on the “experimental” Adler function. The main quantity employed in our analysis is the vector (non-strange) spectral function $v_1(s)$. It is related with the vector invariant mass squared distribution (the function $sfm2(s)$ in the notations of [10])

$$v_1(s) = \kappa(s) sfm2(s), \quad (64)$$

the kinematical factor $\kappa(s)$ is

$$\kappa(s) = \mathcal{N} \frac{m_\tau^2}{(6|V_{ud}|^2 S_{EW})} \left(\frac{B_V}{B_e} \right) \frac{1}{(1 - s/m_\tau^2)^2 (1 + 2s/m_\tau^2)}, \quad (65)$$

where $|V_{ud}| = 0.9746 \pm 0.0006$ denotes the flavor mixing matrix elements, the factor $S_{EW} = 1.0198 \pm 0.0006$ is an electro-weak correction term, $m_\tau = 1777.03_{-0.26}^{+0.3} \text{ MeV}$, $B_V = (31.82 \pm 0.22)\%$ and $B_e = (17.810 \pm 0.039)\%$ are the vector and leptonic branching fractions respectively (in this paper, we assume these estimates following [9]), \mathcal{N} is the normalizing constant

$$\mathcal{N} = \left\{ \int_0^{m_\tau^2} sfm2(s) ds \right\}^{-1} \approx \frac{1}{0.794748}.$$

The quantity $sfm2(s)$ is measured at 140 equidistant values of the energy squared variable starting from $s_1 = 0.0125 \text{ GeV}^2$ with the bin size $\Delta_{bin} = 0.025 \text{ GeV}^2$. Note that the factor $\kappa(s)$

Table 13 A few measured values of $sfm2(s)$ and $v_1(s)$. The standard errors for these quantities are indicated.

$s \text{ GeV}^2$	$sfm2(s)$	$\sigma_{sfm2}(s)$	$v_1(s)$	$\sigma_{v_1}(s)$
0.0875	0.004923	0.001251	0.006027	0.001531
0.1125	0.022630	0.003092	0.027745	0.003791
0.1375	0.037048	0.004520	0.045504	0.005551
0.1625	0.056542	0.005747	0.069597	0.007074
0.1875	0.073407	0.005875	0.090583	0.007250
0.2125	0.095429	0.006541	0.118095	0.008095
0.2375	0.122440	0.007574	0.152005	0.009403

is determined within an accuracy of less than 1% for all values of s in the range $s = 0 - m_\tau^2$, while the errors in determination of $sfm2(s)$ are considerably large. Hence, it is safe to ignore the uncertainties coming from the factor $\kappa(s)$. We may then write

$$\sigma_{v_1}[k] = |\kappa(s_k)|\sigma_{sfm2}[k], \quad k = 1, \dots, 140 \quad (66)$$

where $\sigma_{v_1}[k]$ and $\sigma_{sfm2}[k]$ stand for the standard deviations of $v_1(s_k)$ and $sfm2(s_k)$ respectively, and $s_k = s_1 + (k-1)\Delta_{bin}$ ($k=1, 2, \dots$). By definition

$$\sigma_{v_1}^2[k] = \mathbf{E}[(v_1(s_k) - \overline{v_1(s_k)})^2], \quad (67)$$

etc ¹⁶. Similarly, the covariance matrices of the errors associated with the quantities $v_1(s)$ and $sfm2(s_k)$ are related by the formula

$$\mathbb{C}_{ik} = \kappa(s_i)\kappa(s_k)\tilde{\mathbb{C}}_{ik}, \quad (68)$$

where $\mathbb{C}_{ik} = \text{cov}(v_1(s_i), v_1(s_k))$ and $\tilde{\mathbb{C}}_{ik} = \text{cov}(sfm2(s_i), sfm2(s_k))$. So that respective correlation coefficients coincide

$$\mathbb{R}_{kl} = \frac{\mathbb{C}_{kl}}{\sigma_{v_1}[k]\sigma_{v_1}[l]} = \frac{\tilde{\mathbb{C}}_{kl}}{\sigma_{sfm2}[k]\sigma_{sfm2}[l]}. \quad (69)$$

In Table 13, we present a few measured values of $sfm2(s)$ and $v_1(s)$ together with the associated uncertainties. Our goal is to estimate the uncertainties on the extracted values of the parameters induced from the experimental uncertainties of the spectral function. We start from the system of (39)-(40), which we rewrite in the form

$$\Phi_1(x, y) = \mathcal{E}_1(x, \{v_1\}) \quad (70)$$

$$\Phi_2(x, y) = \mathcal{E}_2(x, \{v_1\}) \quad (71)$$

where we have introduced the notations $x = s_p$, $y = \Lambda^2$ and

$$\begin{aligned} \mathcal{E}_1(x, \{v_1\}) &= \int_0^x v_1(t) dt \\ \mathcal{E}_2(x, \{v_1\}) &= \int_x^{m_\tau^2} w_\tau(t) v_1(t) dt, \end{aligned}$$

to avoid a cumbersome notation the superscript “exp.” in function $v_1^{\text{exp.}}(s)$ has been omitted. The solution to the system (70)-(71) should be considered as a functional of $v_1(s)$. Let a solution for the parameters, for a given function $v_1(s)$, is

$$x = \psi_1(\{v_1\}) \quad (72)$$

$$y = \psi_2(\{v_1\}). \quad (73)$$

¹⁶ The symbol $\mathbf{E}[x]$ refers to the mean value of x .

we may write $v_1(s) = \bar{v}_1(s) + \delta v_1(s)$, where $\bar{v}_1(s)$ is the central (average) value and $\delta v_1(s)$ is the deviation. The central values of the parameters should be determined by solving the system (70)-(71) for $v_1(x) = \bar{v}_1(x)$ (see, for example, the book [68]) i.e.

$$\bar{x} = \psi_1(\{\bar{v}_1\}) \quad (74)$$

$$\bar{y} = \psi_2(\{\bar{v}_1\}). \quad (75)$$

Let us expand the functionals $\mathcal{E}_{1,2}(x, \{v_1\})$ in powers of a small variation $\delta v_1(s)$, preserving the terms linear in δx and $\delta v_1(s)$

$$\mathcal{E}_1(x, \{v_1\}) = \Phi_1(\bar{x}, \bar{y}) + \delta x \bar{v}_1(\bar{x}) + \int_0^{\bar{x}} \delta v_1(t) dt + \dots \quad (76)$$

$$\mathcal{E}_2(x, \{v_1\}) = \Phi_2(\bar{x}, \bar{y}) - w_\tau(\bar{x}) \bar{v}_1(\bar{x}) \delta x + \int_{\bar{x}}^{m_\tau^2} w_\tau(t) \delta v_1(t) dt + \dots, \quad (77)$$

here use has been made of the equations $\mathcal{E}_{1,2}(\bar{x}, \{\bar{v}_1\}) = \Phi_{1,2}(\bar{x}, \bar{y})$. Insert these expansions into Eqs.(70)-(71) and expand the left hand sides of the equations in powers of δx and δy

$$\Phi_{1,2}(x, y) = \Phi_{1,2}(\bar{x}, \bar{y}) + \frac{\partial \Phi_{1,2}(\bar{x}, \bar{y})}{\partial \bar{x}} \delta x + \frac{\partial \Phi_{1,2}(\bar{x}, \bar{y})}{\partial \bar{y}} \delta y + \dots$$

Retaining terms linear in δx , δy and δv_1 , we are led to the following linear algebraic system of equations for the variations δx and δy

$$\begin{aligned} A_1 \delta x + B_1 \delta y &= G_1 \\ A_2 \delta x + B_2 \delta y &= G_2, \end{aligned} \quad (78)$$

where

$$\begin{aligned} A_1 &= \frac{\partial \Phi_1(\bar{x}, \bar{y})}{\partial \bar{x}} - \bar{v}_1(\bar{x}), \quad B_1 = \frac{\partial \Phi_1(\bar{x}, \bar{y})}{\partial \bar{y}}, \quad G_1 = \int_0^{\bar{x}} \delta v_1(t) dt, \\ A_2 &= \frac{\partial \Phi_2(\bar{x}, \bar{y})}{\partial \bar{x}} + w_\tau(\bar{x}) \bar{v}_1(\bar{x}), \quad B_2 = \frac{\partial \Phi_2(\bar{x}, \bar{y})}{\partial \bar{y}}, \quad G_2 = \int_{\bar{x}}^{m_\tau^2} w_\tau(t) \delta v_1(t) dt. \end{aligned}$$

Using the explicit formulas (41) and (42), after some algebra, we obtain

$$\begin{aligned} \frac{\partial \Phi_1(x, y)}{\partial x} &= \frac{(1 + r(x))}{2} \\ \frac{\partial \Phi_1(x, y)}{\partial y} &= \frac{1}{2\pi} \int_{-\infty}^{\ln(x/y)} \tilde{\rho}_{\text{eff}}(t) e^t dt + \frac{c_L}{2} \\ \frac{\partial \Phi_2(x, y)}{\partial x} &= -\frac{(1 + r(x))}{4m_\tau^2} P\left(\frac{x}{m_\tau^2}\right) \\ \frac{\partial \Phi_2(x, y)}{\partial y} &= \frac{1}{4\pi m_\tau^2} \int_{\ln(x/y)}^{\ln(m_\tau^2/y)} \tilde{\rho}_{\text{eff}}(t) e^t P\left(\frac{ye^t}{m_\tau^2}\right), \end{aligned}$$

where $\tilde{\rho}_{\text{eff}}(t) \equiv \rho_{\text{eff}}(\sigma)$ with $\sigma = \Lambda^2 \exp(t)$, $P(z) = 2(z-1)^2(2z+1)$, and $r(s)$ is defined in (23). After solving the system (78), we take the averages of the deviations squared (the variances)

$$\begin{aligned} \overline{(\delta x)^2} &= (B_2^2 \overline{G_1^2} + B_1^2 \overline{G_2^2} - 2B_1 B_2 \overline{G_1 G_2}) / \mathcal{D}^2 \\ \overline{(\delta y)^2} &= (A_1^2 \overline{G_2^2} + A_2^2 \overline{G_1^2} - 2A_1 A_2 \overline{G_1 G_2}) / \mathcal{D}^2, \end{aligned} \quad (79)$$

where $\mathcal{D} = A_1 B_2 - A_2 B_1$, and the overlined symbols refer to the averages: $\overline{(\delta x)^2} = E[(x - \bar{x})^2]$ etc. To calculate the averages $\overline{G_1^2}$, $\overline{G_2^2}$ and $\overline{G_1 G_2}$ we replace the integrals $G_{1,2}$ by sums over the equidistant mesh, using the trapezoidal rule,

$$G_1 \approx \Delta \sum_{k=1}^{n_p} g_k \delta v_1(t_k), \quad G_2 \approx \Delta \sum_{k=n_p}^{n_\tau} \eta_k \delta v_1(t_k) \quad (80)$$

where $n_p = 1 + [(\bar{s}_p - s_1)/\Delta]_{\text{round}}$, $n_\tau = 1 + [(m_\tau^2 - s_1)/\Delta]_{\text{round}}$ ¹⁷, Δ denotes the width of the mesh which is identified with the bin size in the data. The mesh points in the sums are determined by $t_k = t_1 + (k-1)\Delta$, $k = 1, 2, \dots$, with $t_1 = 0.0125$ and $\Delta = 0.025$. The numerical coefficients g_k take the values $g_k = 1$ for $1 < k < n_p$ and $g_1 = g_{n_p} = 0.5$. The factors η_k are determined by

$$\begin{cases} \eta_k = w_\tau(t_k) & \text{if } n_p < k < n_\tau. \\ \eta_k = 0.5w_\tau(t_k) & \text{if } k = n_p \text{ or } k = n_\tau. \end{cases}$$

Using formula (80) and taking into account the definitions (67) and (68), we calculate the required averages

$$\overline{G_1^2} = (\Delta)^2 \left(\sum_{k=1}^{n_p} g_k^2 \sigma_{v_1}^2[k] + 2 \sum_{k=1}^{n_p-1} \sum_{l>k}^{n_p} g_k g_l \mathbb{C}_{kl} \right), \quad (81)$$

$$\overline{G_2^2} = (\Delta)^2 \left(\sum_{k=n_p}^{n_\tau} \eta_k^2 \sigma_{v_1}^2[k] + 2 \sum_{k=n_p}^{n_\tau-1} \sum_{l=k+1}^{n_\tau} \eta_k \eta_l \mathbb{C}_{kl} \right), \quad (82)$$

$$\overline{G_1 G_2} = (\Delta)^2 \sum_{k=1}^{n_p} \sum_{l=n_p}^{n_\tau} g_k \eta_l \mathbb{C}_{kl}. \quad (83)$$

We are now in a position to determine the uncertainties on the values of the “experimental” Adler function. They are induced from the errors of the experimental spectral function and from the errors on the parameters Λ and s_p . Let us represent again the “experimental” Adler function as a sum of the two terms showing explicitly the dependence of the terms on the parameters and on the spectral function

$$D_{\text{“exp”}}(Q^2, \Lambda^2, s_p : v_1) = D_{\text{exp}}(Q^2, s_p : v_1) + D_{\text{pQCD}}(Q^2, \Lambda^2, s_p), \quad (84)$$

the experimental and pQCD parts of the function are determined as

$$D_{\text{exp}}(Q^2, s_p : v_1) = \int_0^{s_p} \mathcal{K}(Q^2, t) v_1(t) dt \quad (85)$$

$$D_{\text{pQCD}}(Q^2, \Lambda^2, s_p) = \int_{s_p}^{\infty} \mathcal{K}(Q^2, t) v_1^{\text{APT}}(t) dt, \quad (86)$$

where $\mathcal{K}(Q^2, t) = 2Q^2/(t + Q^2)^2$, $v_1(s)$ denotes the spectral function measured on the experiment ($v_1(s) \equiv v_1^{\text{exp}}(s)$) and $v_1^{\text{APT}}(s)$ is the approximation to the spectral function evaluated within APT. Consider small deviations of the spectral function and the parameters from their mean values

$$v_1(t) = \bar{v}_1(t) + \delta v_1(t), \quad s_p = \bar{s}_p + \delta s_p, \quad \Lambda^2 = \bar{\Lambda}^2 + \delta \Lambda^2, \quad (87)$$

the change of the “experimental” Adler function under these variations is

$$\delta D_{\text{“exp”}} = \delta D_{\text{exp}} + \delta D_{\text{pQCD}}, \quad (88)$$

here we have used abbreviations $D_{\text{exp}} \equiv D_{\text{exp}}(Q^2, s_p : v_1)$ etc. The right hand side of (88) can be evaluated using formulas (85) and (86). Preserving terms linear in the variations δv_1 , δs_p and $\delta \Lambda^2$, we find

$$\delta D_{\text{“exp”}} = \delta v_1 D_{\text{exp}} + E_{\bar{s}_p} \delta s_p + E_{\bar{\Lambda}^2} \delta \Lambda^2 \quad (89)$$

where

$$\delta v_1 D_{\text{exp}} = \int_0^{\bar{s}_p} \mathcal{K}(Q^2, t) \delta v_1(t) dt, \quad (90)$$

$$E_{\bar{s}_p} = \mathcal{K}(Q^2, \bar{s}_p) \bar{v}_1(\bar{s}_p) + \frac{\partial D_{\text{pQCD}}(Q^2, \bar{\Lambda}^2, \bar{s}_p)}{\partial \bar{s}_p}, \quad (91)$$

$$E_{\bar{\Lambda}^2} = \frac{\partial D_{\text{pQCD}}(Q^2, \bar{\Lambda}^2, \bar{s}_p)}{\partial \bar{\Lambda}^2}. \quad (92)$$

¹⁷ here the subscript “round” refers to the integer nearest to the number inside the square bracket.

Using the trapezoidal rule, we approximate the integral on the right side of Eq. (90)

$$\delta_{v_1} D_{\text{exp}} \approx G_3 = \sum_{k=1}^{n_p} g_k \mathcal{K}(Q^2, t_k) \delta v_1(t_k), \quad (93)$$

where the quantities n_p , g_k and t_k are defined below formula (80). To calculate the partial derivatives on the right hand sides of (91) and (92), we use explicit formula (25) for the pQCD part of the Adler function. We then obtain

$$\begin{aligned} \frac{\partial D_{\text{pQCD}}(Q^2, \Lambda^2, s_p)}{\partial s_p} &= -\frac{Q^2}{(Q^2 + s_p)^2} (1 + r(s_p)) \\ \frac{\partial D_{\text{pQCD}}(Q^2, \Lambda^2, s_p)}{\partial \Lambda^2} &= \frac{1}{\pi Q^2} \int_{\ln(s_p/\Lambda^2)}^{\infty} \frac{e^t \tilde{\rho}_{\text{eff}}(t)}{\left(1 + \frac{\Lambda^2}{Q^2} e^t\right)^2} dt, \end{aligned}$$

where $\tilde{\rho}_{\text{eff}}(t) \equiv \rho_{\text{eff}}(\Lambda^2 e^t)$ and to derive the last formula we have used the relation

$$\frac{\partial r(s_p)}{\partial \Lambda^2} = \frac{1}{\pi \Lambda^2} \rho_{\text{eff}}(s_p),$$

which can be easily derived from the definition (23). The mean squared deviation of the “experimental” Adler function is then determined as a sum of the six averages

$$\begin{aligned} \overline{(\delta D_{\text{exp}})^2} &= \overline{(\delta_{v_1} D_{\text{exp}})^2} + E_{\tilde{s}_p}^2 \overline{(\delta s_p)^2} + E_{\Lambda^2}^2 \overline{(\delta \Lambda^2)^2} \\ &\quad + 2E_{\tilde{s}_p} E_{\Lambda^2} \overline{\delta s_p \delta \Lambda^2} + 2E_{\tilde{s}_p} \overline{(\delta_{v_1} D_{\text{exp}}) \delta s_p} + 2E_{\Lambda^2} \overline{(\delta_{v_1} D_{\text{exp}}) \delta \Lambda^2}. \end{aligned} \quad (94)$$

With the aid of formula (93), the first term on the right of Eq. (94) can easily be expressed in terms of the errors σ_{v_1} and the covariance matrix \mathbb{C}_{kl}

$$\overline{(\delta_{v_1} D_{\text{exp}})^2} = \Delta^2 \left\{ \sum_{k=1}^{n_p} g_k^2 \mathcal{K}^2(Q^2, t_k) \sigma_{v_1}^2[k] + 2 \sum_{k=1}^{n_p-1} \sum_{l=k+1}^{n_p} g_k g_l \mathcal{K}(Q^2, t_k) \mathcal{K}(Q^2, t_l) \mathbb{C}_{kl} \right\}. \quad (95)$$

The second and third terms on the right of (94) are determined in terms of the errors σ_{s_p} and σ_{Λ^2} which we have already evaluated above (see (79)). In order to evaluate last three terms on the right of (94), we use explicit expressions for the deviations δs_p and $\delta \Lambda^2$

$$\begin{aligned} \delta s_p &= \mathcal{D}^{-1}(B_2 G_1 - B_1 G_2) \\ \delta \Lambda^2 &= \mathcal{D}^{-1}(A_1 G_2 - A_2 G_1), \end{aligned} \quad (96)$$

the solution to the system (78). This enable us to write

$$\overline{\delta s_p \delta \Lambda^2} = \mathcal{D}^{-2} \{ (B_2 A_1 + B_1 A_2) \overline{G_1 G_2} - B_2 A_2 \overline{G_1^2} - B_1 A_1 \overline{G_2^2} \}, \quad (97)$$

the averages on the right hand side of (97) have been evaluated above (see Eqs. (81), (82) and (83)). It remains to calculate the last two averages on the right hand side of (94). Using formulas (96) we find

$$\overline{(\delta_{v_1} D_{\text{exp}}) \delta s_p} = \overline{G_3 \delta s_p} = \mathcal{D}^{-1} (B_2 \overline{G_1 G_3} - B_1 \overline{G_2 G_3}) \quad (98)$$

$$\overline{(\delta_{v_1} D_{\text{exp}}) \delta \Lambda^2} = \overline{G_3 \delta \Lambda^2} = \mathcal{D}^{-1} (A_1 \overline{G_2 G_3} - A_2 \overline{G_1 G_3}), \quad (99)$$

employing now the trapezoidal sums (80) and (93), we determine the averages $\overline{G_1 G_3}$ and $\overline{G_2 G_3}$ in terms of the correlation coefficients $\mathbb{R}_{k,l}$

$$\begin{aligned} \overline{G_1 G_3} &= \Delta^2 \sum_{k=1}^{n_p} g_k \sigma_{v_1}[k] \sum_{l=1}^{n_p} g_l \mathcal{K}(Q^2, t_l) \mathbb{R}_{k,l} \sigma_{v_1}[l] \\ \overline{G_2 G_3} &= \Delta^2 \sum_{k=n_p}^{n_\tau} \eta_k \sigma_{v_1}[k] \sum_{l=1}^{n_p} g_l \mathcal{K}(Q^2, t_l) \mathbb{R}_{k,l} \sigma_{v_1}[l]. \end{aligned}$$

C Standard CIPT Consideration

It is instructive to compare the modified procedure for extracting the coupling constant with the standard procedure formulated within conventional CIPT in the $\overline{\text{MS}}$ scheme. The τ decay rate to the non-strange hadrons in the vector channel is given by [6]

$$R_{\tau,V} = \frac{3}{2} |V_{ud}|^2 S_{\text{EW}} (1 + \delta_{\text{QCD}} + \delta_{\text{EW}}) \quad (100)$$

where δ_{QCD} represents the QCD corrections, $|V_{ud}| = 0.9746 \pm 0.0006$ is the flavor mixing matrix element, $S_{\text{EW}} = 1.0198$ is an electro-weak correction term and $\delta_{\text{EW}} \approx 0.001$ is an additive electroweak correction (for these values see [9]). The QCD contribution is the sum

$$\delta_{\text{QCD}} = \delta^{(0)} + \delta^{(2)} + \delta_{\text{NP}}, \quad (101)$$

where $\delta^{(0)}$ is the purely perturbative contribution, $\delta^{(2)}$ is the dimension $D = 2$ effects from light quark masses, and δ_{NP} is the total non-perturbative contribution: $\delta_{\text{NP}} = \delta^{(4)} + \delta^{(6)} + \delta^{(8)}$ ($\delta^{(D)}$ are the OPE terms in powers of m_τ^{-D}). We will use the estimates $\delta^{(2)} = (-3.3 \pm 3) \times 10^{-4}$ and $\delta_{\text{NP}} = 0.0199 \pm 0.0027$, the ALEPH results obtained within the CIPT approach [9]. The experimental result for $\delta^{(0)}$ can be determined from the experimental spectral function via the relation

$$1 + \delta_{\text{exp}}^{(0)} + \delta^{(2)} + \delta_{\text{NP}} + \delta_{\text{EW}} = 4J_{\tau,V}^{\text{exp}}, \quad (102)$$

where

$$J_{\tau,V}^{\text{exp}} = \int_0^{m_\tau^2} w_\tau(s) v_1^{\text{exp}}(s) ds, \quad (103)$$

and explicit expression of the function $w_\tau(s)$ is given in (36). The relation (102) follows from formulas (36) and (100). Let us now determine the experimental error on $J_{\tau,V}^{\text{exp}}$ induced from the experimental errors on $v_1^{\text{exp}}(s)$. Using the trapezoidal rule, we replace the integral on the right side of Eq. (103) by the sum

$$J_{\tau,V}^{\text{exp}} \approx \Delta \sum_{k=1}^{N_\tau} g_k w_\tau(s_k) v_1(s_k) \quad (104)$$

where $N_\tau = 1 + [(m_\tau^2 - s_1)/\Delta]_{\text{round}}$, $s_k = s_1 + (k-1)\Delta$ with $s_1 = 0.0125$ and $\Delta = 0.025$, and g_k are the numeric coefficients associated with the trapezoidal rule. From formula (104) one easily evaluates the standard error on $J_{\tau,V}^{\text{exp}}$

$$\sigma(J_{\tau,V}^{\text{exp}}) = \Delta \left[\sum_{k=1}^{N_\tau} \sum_{n=1}^{N_\tau} g_k g_n w_\tau(s_k) w_\tau(s_n) \mathbb{C}_{k,n} \right]^{\frac{1}{2}} \quad (105)$$

where \mathbb{C} denotes the covariance matrix $\mathbb{C}_{i,k} = \mathbf{E}[(v_1(s_i) - \overline{v_1(s_i)})(v_1(s_k) - \overline{v_1(s_k)})]$ which is available in [10]. It follows from Eqs. (101) and (102) that

$$\sigma(\delta_{\text{QCD}}) = [\sigma^2(\delta^{(0)}) + \sigma^2(\delta_{\text{NP}})]^{1/2} = 4\sigma(J_{\tau,V}^{\text{exp}}), \quad (106)$$

where we have ignored the small correlation between $\delta^{(0)}$ and δ_{NP} . With the data provided by ALEPH [10], from Eqs. (102), (105) and (106) we obtain ¹⁸

$$\delta_{\text{exp}}^{(0)} = 0.2091 \pm 0.0065_{\text{exp}}, \quad (107)$$

it should be noted that in [12] slightly large value and error have been obtained, namely, $\delta_{\text{exp}}^{(0)} = 0.2093 \pm 0.008_{\text{exp}}$. The perturbative QCD correction obtained within CIPT is represented via

¹⁸ Alternatively, we could have determined the error on $\delta_{\text{exp}}^{(0)}$ directly from the known error on $R_{\tau,V}$ using formula (100) with the estimate $\delta_{\text{NP}} = 0.0199 \pm 0.0027$.

Table 14 Numerical values for the QCD scale parameter and strong coupling constant in the $\overline{\text{MS}}$ scheme for three active flavours extracted from the non-strange vector τ lepton data within the conventional CIPT approach. The results obtained in consecutive orders of perturbation theory are given. The error bars refer to the experimental uncertainty only.

Perturbative orders	Λ GeV	$\alpha_s(m_\tau^2)$
LO	0.604 ± 0.023	0.485 ± 0.019
NLO	0.469 ± 0.018	0.390 ± 0.011
N ² LO	0.430 ± 0.016	0.367 ± 0.009
N ³ LO	0.407 ± 0.015	0.354 ± 0.008
N ⁴ LO	0.395 ± 0.015	0.347 ± 0.008

the contour integral in the complex momentum squared plane [23,24]. This integral can be rewritten as

$$\delta_{\text{CI}}^{(0)} = \frac{1}{\pi} \int_0^\pi \text{Re} \left\{ (1 - e^{i\varphi}) (1 + e^{i\varphi})^3 d_{\text{RGI}}(s_0 e^{i\varphi}) \right\} d\varphi, \quad (108)$$

where $s_0 = m_\tau^2$ and $d_{\text{RGI}}(z)$ denote the RG improved perturbative correction to the Adler function defined in (14). To calculate $d_{\text{RGI}}(z)$, usually, the four-loop order RG equation is solved numerically for the running coupling. We find convenient to use the implicit solution to the RG equation at the four-loop order (relevant formulas can be found in [33]). The running coupling satisfies a transcendental equation which is solved numerically. To extract the value of the QCD scale parameter $\Lambda \equiv \Lambda_{\overline{\text{MS}}}$, one solves the equation

$$\delta_{\text{CI}}^{(0)}(\Lambda) = \delta_{\text{exp}}^{(0)}. \quad (109)$$

Numerical values for the QCD scale parameter and strong coupling constant (for $n_f = 3$ number of flavours) extracted from the experimental value (107) are given in Table 14. We have used various approximations to the Adler function evaluated with the four-loop running coupling. For the unknown N⁴LO coefficient of the Adler function, we have used the geometric series estimate $d_5 \approx 378 \pm 378$ [12].

References

1. Bertlmann, R.A., Launer, G. and de Rafael, E.: Gaussian sum rules in quantum chromodynamics and local duality. Nucl. Phys. B250 (1985) 61.
2. de Rafael, E.: An Introduction to sum rules in QCD. Lectures at the Les Houches Summer School 1997. arXiv: 9802448 [hep-ph]
3. Peris, S., Perrottet, M., de Rafael, E.: Matching long and short distances in large- N_c QCD. JHEP **9805**, 011 (1998)
4. Shifman, M.A., Vainshtein, A.I., Zakharov, V.I.: QCD and resonance physics. Theoretical foundations. Nucl. Phys. B **147**, 385 (1979)
5. Poggio, E.C., Quinn, H.R., Wainberg, S.: Smearing method in the quark model. Phys. Rev.D **13** 1958-1968 (1976)
6. Braaten, E., Narison, S., and Pich, A.: QCD analysis of the tau hadronic width. Nucl. Phys. B **373**, 581 (1992)
7. Shifman, M.A.: Quark-hadron duality. Boris Ioffe Festschrift. At the Frontier of Particle Physics, Handbook of QCD, M. A. Shifman (ed.) World Scientific Singapore (2001)
8. Peris, S., Phily, B., de Rafael, E.: Tests of Large- N_c QCD from Hadronic τ Decay. Phys. Rev. Lett. **86**, 14-17 (2001)
9. Schael, S. et al.: Branching ratios and spectral functions of τ decays: Final ALEPH measurements and physics implications [ALEPH Collaboration]. Phys. Rept. **421**, 191 (2005)
10. The ALEPH data for the spectral functions is available at <http://aleph.web.lal.in2p3.fr/tau/specfun.html>.
11. Davier, M., Höcker, A., Zhang, Z.: The physics of hadronic tau decays. Rev. Mod. Phys. **78** 1043 (2006)
12. Davier, M., Höcker, A.H., Zhang, Z.: The determination of α_s from τ decays revisited. Eur. Phys. J. C **56**, 305-322 (2008)
13. Mason, Q. et al.: Accurate determinations of α_s from realistic lattice QCD. Phys. Rev. Lett. **95**052002 (2005)
14. Maltman, K., Yavin, T.: $\alpha_s(M_\tau^2)$ from hadronic τ decays. Phys. Rev. D **78** 094020 (2008)
15. Dominguez, C.A., Nasrallah, N.F., Schilcher, K.: Confronting QCD with the experimental hadronic spectral functions from tau-decay. Phys. Rev. D **80**, 054014, (2009)
16. Dominguez, C.A., Schilcher, K.: QCD vacuum condensates from tau-lepton decay data. JHEP **0701** 093, (2007)
17. Gonzales-Alonso, M., Pich, A., Prades, J.: Pinched weights and duality violations in QCD sum rules: a critical analysis. Phys. Rev. D **82**, 014019, (2010)
18. Narison, S.: Power corrections to $\alpha_s(M_\tau)$, $|V_{us}|$ and \bar{m}_s . Phys. Lett. B **673**, 30-36 (2009)
19. Cata, O., Golterman, M., Peris, S.: Unraveling duality violations in hadronic tau decays. Phys. Rev. D **77**, 093006 (2008)
20. Cata, O., Golterman, M., Peris, S.: Possible duality violations in τ decay and their impact on the determination of α_s . Phys. Rev. D **79**, 053002 (2009)
21. Boito, D. et.al.: A new determination of α_s from hadronic τ decays. arXiv: 1110.1127 [hep-ph] (2011)
22. Pivovarov, A.A.: Sov. J. Nucl. Phys. **54**, 676 (1991)
23. Pivovarov, A.A.: Renormalization group analysis of the τ -lepton decay within QCD. Z. Phys. C **53** 461-464 (1992) [hep-ph/0302003].
24. Le Diberger F., Pich A.: The perturbative QCD prediction to R_τ revisited. Phys. Lett. B **286**, 147-152 (1992)
25. Jamin, M.: Contour-improved versus fixed-order perturbation theory in hadronic tau decays. JHEP **0509**, 058 (2005)
26. Beneke, M., Jamin, M.: α_s and the τ hadronic width: fixed-order, contour-improved and higher-order perturbation theory. JHEP **0809**, 044 (2008)
27. Körner, J.G., Krajewski, F., Pivovarov, A.A.: Strong coupling constant from τ decay within a renormalization scheme invariant treatment. Phys. Rev. D **63**, 036001 (2001)
28. Kataev, A.L., Starshenko, V.V.: Estimates of the higher-order QCD corrections to $R(s)$, R_τ and deep inelastic scattering sum rules. Mod. Phys. Lett. A **10**, 235 (1995)
29. Raczka, P.A.: Towards more reliable perturbative QCD predictions at moderate energies. arXiv: hep-ph/0602085 (2006)
30. Gardi, E., Grunberg, G., Karliner, M.: Can the QCD running coupling have a causal analyticity structure? J. High Energy Phys. **07**, 007 (1998)

31. Magradze, B.A.: The gluon propagator in analytic perturbation theory. In: Proceedings of the 10th International Seminar "QUARKS-98" Suzdal, Russia, 1998 (Bezrukov F. L., et al.: eds.), vol 1, p. 158, Moscow: Russian Academy of Sciences, Institute for Nuclear Research 1999
32. Magradze, B.A.: An analytic approach to perturbative QCD. *Int. J. Mod. Phys. A* **15**, 2715 (2000)
33. Magradze, B.A.: A novel series solution to the renormalization group equation in QCD. *Few-Body Systems* **40**, 71-99 (2006)
34. Krasnikov, A.N., Pivovarov, A.A.: Renormalization schemes and renormalons. *Mod. Phys. Lett. A* **11**, 835 (1996)
35. Shirkov, D.V., Solovtsov, I.L.: Analytic model for the QCD running coupling with universal $\bar{\alpha}_s(0)$ Value. *Phys. Rev. Lett.* **79**, 1209 (1997)
36. Dokshitzer, Yu., Marchesini, G., Webber, B.R.: Dispersive Approach to Power-Behaved Contributions in QCD Hard Processes. *Nucl. Phys. B* **469**, 93 (1996)
37. Grunberg, G.: On power corrections in the dispersive approach. *JHEP* **9811**, 006 (1998)
38. Milton, K.A., Solovtsov, I.L., Solovtsova, O.P.: Analytic perturbation theory and inclusive tau Decay. *Phys. Lett. B* **415**, 104 (1997)
39. Milton, K.A., Solovtsov, I.L., Solovtsova, O.P., Yasnov, V.I.: Renormalization scheme and higher loop stability in hadronic tau decay within analytic perturbation theory. *Eur. Phys. J. C* **14**, 495-501 (2000)
40. Solovtsov, I.L., Shirkov, D.V.: Analytic approach in quantum chromodynamics. *Theor. Math. Phys.* **120**, 1220 (1999)
41. Shirkov, D.V.: Analytic perturbation theory in analyzing some QCD observables. *Eur. Phys. J. C* **22**, 331 (2001)
42. Shirkov, D. V.: *Lett. Math. Phys.* **48**, 135 (1999)
43. Shirkov, D.V., Solovtsov, I.L.: Ten years of the Analytic Perturbation Theory in QCD. *Theor. Math. Phys.* **150** 132-152 (2007)
44. Milton, K.A., Solovtsova, O.P.: Perturbative expansions in the inclusive decay of the tau lepton. *Int. J. Mod. Phys. A* **17**, 3789 (2002)
45. Milton, K.A., Solovtsov, I.L., O.P. Solovtsova, O.P.: The Adler Function for Light Quarks in Analytic Perturbation Theory. *Phys. Rev. D* **64** 016005 (2001)
46. Shirkov, D.V., Large regular QCD coupling at low energy? Published in Tegernsee 2008, Quantum field theory and beyond, pp. 34-45, arXiv: 0807.1404 [hep-ph] (2008)
47. Cvetič, G., Valenzuela, C., Schmidt, I.: A modification of minimal analytic QCD at low energies. arXiv: 0508101 [hep-ph] (2005)
48. Contreras, C., et al.: Simple analytic QCD model with perturbative QCD behavior at high momenta. *Phys. Rev. D* **82** 074005 (2010)
49. Bakulev, A.P., Mikhailov, S.V., Stefanis, N.G.: QCD Analytic Perturbation Theory. From integer powers to any power of the running coupling. *Phys. Rev. D* **72**, 074014 (2005)
50. Bakulev, A.P., Mikhailov, S.V., Stefanis, N.G.: Higher-order QCD perturbation theory in different schemes: From FOPT to CIPT to FAPT. *JHEP* **1006** 085 (2010)
51. Bakulev A.P., Shirkov D.V.: Inevitability and importance of non-perturbative elements in quantum field theory. arXiv: 1102.2380 [hep-ph] (2011)
52. Prosperi, G.M., Raciti, M., Simolo, C.: On the running coupling constant in QCD. *Prog. Part. Nucl. Phys.* **58**, 387-438 (2007)
53. R. Barate et. al.: Measurement of the axial-vector τ spectral functions and determination of $\alpha_s(M_Z^2)$ [ALEPH Collaboration]. *Eur. Phys. J. C* **4**, 409-431 (1998)
54. K. Ackerstaff, K., et al. Measurements of the strong coupling constant α_s and the vector and axial vector spectral functions in hadronic tau decays. [OPAL Collaboration] *Eur. Phys. J. C* **7**, 571 (1999)
55. Eidelman, S., Jagerlehner, F., Kataev, A.L., Veretin O.: Testing non-perturbative strong interaction effects via the Adler function. *Phys. Lett. B* **454**, 369-380 (1999)
56. Chetyrkin, K.G., Kataev, A.L., Tkachov F.V.: Higher Order Corrections to $\sigma_t(e^+ + e^- \rightarrow \text{Hadrons})$ in Quantum Chromodynamics. *Phys. Lett. B* **85**, 277 (1979)
57. Gorishnii, S.G., Kataev, A.L., Larin, S.A.: The $O(\alpha_s^3)$ corrections to $\sigma_{tot}(e + e^- \rightarrow \text{hadrons})$ and $\Gamma(\tau \rightarrow \text{tau-neutrino} + \text{hadrons})$ in QCD. *Phys. Lett. B* **259** 144-150 (1991)
58. Surguladze L.R., Samuel, M.A.: Total hadronic cross-section in $e^+ e^-$ annihilation at the four loop level of perturbative QCD. *Phys. Rev. Lett.* **66** 560-563 (1991) (1991 Erratum-ibid. **66**, 2416 (1991))
59. Baikov, P.A., Chetyrkin, K.G., Kühn, J.H.: Hadronic Z- and tau-Decays in Order α_s^4 . *Phys. Rev. Lett.* **101** 012002, (2008)

-
- 60. Chetyrkin, K.G., Kühn, J.H., Kwiatkowski, A.: QCD corrections to the e^+e^- cross-section and the Z boson decay rate: concepts and results. *Phys. Rep.* **277** 189-281 (1996)
 - 61. Kourashev, D.S.: The QCD observables expansion over the scheme-independent two-loop coupling constant powers, the scheme dependence reduction. arXiv: 9912410 [hep-ph] (1999)
 - 62. Kourashev, D.S., Magradze, B.A.: Explicit expressions for Euclidean and Minkowskian QCD observables in analytic perturbation theory. *Theor. Math. Phys.* **135**, 531 (2003)
 - 63. Girone, M., Neubert, M.: Test of the running of α_s in τ decays. *Phys. Rev. Lett.* **76** 3061-3064 (1996)
 - 64. Rodrigo, G., Santamaria, A.: QCD Matching Conditions at Thresholds. *Phys. Lett. B* **313** 441-446 (1993)
 - 65. Chetyrkin, K.G., Kniehl, B.A., Steinhauser, M.: Strong Coupling Constant with Flavour Thresholds at Four Loops in the $\overline{\text{MS}}$ Scheme. *Phys. Rev. Lett.* **79** 2184-2187 (1997)
 - 66. Rodrigo, G., Pich A., Santamaria A.: $\alpha_s(m_Z)$ from tau decays with matching conditions at three loops. *Phys. Lett. B* **424** 367-374 (1998)
 - 67. Yao, W.-M., et al.: Review of Particle Physics (The Particle Data Group). *J. Phys. G* **33**,1 (2006)
 - 68. Hudson, Derek J.: Lectures on Elementary Statistics and Probability. Pages 101, publisher CERN, Geneva (1963)
 - 69. Van Ritberger, T., Vermaseren, J.A.M., Larin, S.A.: The four-loop β -function in Quantum Chromodynamics. *Phys. Lett B* **400**, 379 (1997)
 - 70. Corless, R.M., et al.: On the Lambert W function. *Advances in Computation Mathematics* **5**, 329 (1996).